

LEVOGLUCOSAN TRANSFORMATION AND KINETICS OF HEMICELLULOSE  
HYDROLYSIS USING CARBON SUPPORTED SOLID ACID CATALYSTS

by

RICHARD V. ORMSBY

(Under the Direction of James R. Kastner)

ABSTRACT

Reusable carbon based solid acid catalysts are less expensive and potentially more sustainable than enzymatic and liquid acid catalysts used in biomass conversion processes utilized in a commercial biorefinery. Sulfonated pine chip biochar catalyst effectively hydrolyzed model xylan (hemicellulose) and levoglucosan into xylose and glucose in small bench scale bio-reactors with a maximum yield (compared to a liquid acid catalyst) of approximately 88% and 80% conversion respectively after 2 hours at 120 °C. Fast pyrolysis oil was used to generate a concentrated levoglucosan feedstock. Simultaneous hydrolysis and esterification of fast-pyrolysis bio-oil resulted in the generation of glucose, ethers, and esters, but in lower concentration compared to model compound experimentation.

INDEX WORDS: Biochar, hemicellulose, levoglucosan, biorefinery, solid acid catalyst

LEVOGLUCOSAN TRANSFORMATION AND KINETICS OF HEMICELLULOSE  
HYDROLYSIS USING CARBON SUPPORTED SOLID ACID CATALYSTS

by

RICHARD V. ORMSBY

B.S., The University of Georgia, 2008

A Thesis Submitted to the Graduate Faculty of The University of Georgia in Partial  
Fulfillment of the Requirements for the Degree

MASTER OF SCIENCE

ATHENS, GEORGIA

2011

© 2011

RICHARD V. ORMSBY

All Rights Reserved

LEVOGLUCOSAN TRANSFORMATION AND KINETICS OF HEMICELLULOSE  
HYDROLYSIS USING CARBON SUPPORTED SOLID ACID CATALYSTS

by

RICHARD V. ORMSBY

Major Professor: James R. Kastner  
Committee: Sudhagar Mani  
Keshav C. Das

Electronic Version Approved:

Maureen Grasso  
Dean of the Graduate School  
The University of Georgia  
December 2011

## **DEDICATION**

To my son, Raylan Robert Ormsby, you make my world a better place. I will spend my life loving you and trying to make your world even better.

To my wife, Andrea Michelle Ormsby, you are my dearest friend and ally. Your continuous love and support strengthens my belief that we can achieve anything together. I'll never dance half as well without you.

To my sister, Kimberly Robin Daniel, you are the most ferociously loyal person I have ever met. The strength required for anyone to care half as much as you do never ceases to impress me.

To my mother, Robin Ormsby Daniel, I found the joy of asking questions and seeking answers because of you. Your unending love and guidance are gifts that I cannot repay, but strive to give to my own children.

To my aunt, Marka Robin Ormsby, you never allowed the word "extended" to be placed next to "family." Thank you for always being available through every stage of my life and providing us all with such a close family.

To my grandfather, Robert Benzein Ormsby Jr., you are truly a gentleman and a scholar. I know what it means to be a good man because of you. It is forever my goal to live up to your example as a father, a friend, and an engineer.

To my grandmother, Margaret Williams Ormsby, you let me know what it feels like to be the apple of someone's eye. I miss you.

## ACKNOWLEDGEMENTS

I would like to acknowledge the many contributions of Dr. James R. Kastner. If not for his knowledge and guidance, this work would not be possible. His door was always open and he never hesitated to welcome my thoughts and questions with an open mind. I would like to thank him for his incredible thoughtfulness and unwavering encouragement throughout my entire graduate career. I would also like to thank Dr. K. C. Das and Dr. Sudhagar Mani for their questions, insight, encouragement, and patience throughout my research.

I would like to acknowledge the equally significant contributions of Joby Miller. Her dedication and tenacity for solving problems helped this work prevail in the face of all obstacles. I would like to thank her for always lending both hands even when they were full, and suffering with me through the slings and arrows of working with an RT-elite welled hot plate. She has truly been an amazing friend and ally.

I would also like to acknowledge the assistance of Roger Hilten, Sarah Lee, Darcy Lichlyter, and Keith Harris. I would like to thank Roger for his fast-pyrolysis reactor and keeping me supplied throughout my research. I would like to thank Sarah on behalf of all engineering graduate students for keeping the HPLC working at all hours. I would like to thank Darcy and Keith for their wit, good cheer, and positive attitude in addition to all of their help repairing and maintaining the underappreciated Dionex ion chromatograph.

Finally I would like to thank Dr. William Tollner, Dr. Sid Thompson, and Dr. Dale Threadgil for their encouragement and the opportunity to teach while learning.

## TABLE OF CONTENTS

	Page
ACKNOWLEDGEMENTS .....	v
LIST OF TABLES .....	ix
LIST OF FIGURES .....	x
CHAPTER	
1 INTRODUCTION .....	1
2 HYPOTHESIS AND OBJECTIVES .....	5
Hypothesis.....	5
Objectives .....	5
3 LITERATURE REVIEW .....	7
Hemicellulose Extraction.....	7
Liquid Acid and Enzymatic Catalysts.....	9
Solid Acid Catalysts.....	9
Biochar Supported Solid Acid Catalysts.....	11
Hemicellulose Hydrolysis Kinetics.....	12
Levoglucosan Extraction .....	13
Levoglucosan Hydrolysis.....	13
4 MATERIALS AND METHODS.....	16
Model Compounds.....	16
Biochar Synthesis and Sulfonation .....	16

	Activated Carbon Sulfonation.....	17
	Analytical Methods.....	18
	Hemicellulose Hydrolysis.....	21
	Amberlyst 15 Resin.....	23
	Hemicellulose Hydrolysis Kinetics.....	23
	Fast Pyrolysis Oil.....	24
	Levoglucosan Hydrolysis.....	26
	Simultaneous Esterification and Hydrolysis.....	26
5	HEMICELLULOSE RESULTS AND DISCUSSION.....	28
	Catalyst Characterization.....	28
	Hemicellulose Hydrolysis with PCC Catalyst.....	32
	Reuse PCC Hemicellulose Hydrolysis.....	35
	Hemicellulose Hydrolysis with AC Catalyst.....	36
	Hemicellulose Hydrolysis with Amberlyst 15 Resin.....	37
	Reuse A15R Hemicellulose Hydrolysis.....	39
	Reaction Rate and Agitation.....	41
	Hemicellulose Reaction Kinetics.....	42
6	LEVOGLUCOSAN RESULTS AND DISCUSSION.....	48
	PCC Hydrolysis of Model Levoglucosan.....	48
	Bio-oil Characterization.....	50
	Bio-oil Hydrolysis with PCC.....	51
7	CONCLUSIONS AND FUTURE RESEARCH.....	58
	Hemicellulose.....	58

Levogluconan and Bio-oil.....	59
REFERENCES .....	61
APPENDICES	
A HPLC Standard Curve Generation.....	64
B Complete Acid Hydrolysis Calculations.....	67

## LIST OF TABLES

	Page
Table 1: Sulfonated PCC sulfur composition (CHNS analysis).....	28
Table 2: Physical characteristics of biochar and catalysts .....	31
Table 3: A15R sulfonic characteristics (CHNS analysis) and PCC comparison.....	39
Table 4: Reaction rate of xylan hydrolysis with PCC and A15R catalysts.....	46
Table 5: Initial sugar concentrations for aqueous and non aqueous phase FP oil .....	51
Table 6: ILC-Bio-oil hydrolysis product yield concentrations at various time intervals at 123 °C .....	52
Table 7: Average concentration of fast-pyrolysis oil compounds before and after hydrolysis with solid acid catalysts.....	54
Table A.1: HPLC retention times .....	66
Table B.1: Xylose recovery and xylan hydrolysis data for the calculation of xylose content.....	68
Table B.2: Average xylose content per unit xylan.....	69

## LIST OF FIGURES

	Page
Figure 1: Flow diagram for the biochemical conversion of lignocellulosic biomass to chemicals and fuels .....	3
Figure 2: Flow diagram for the thermochemical conversion of lignocellulosic biomass to chemicals and fuels.....	3
Figure 3: Reaction pathway for the acid hydrolysis of xylan to xylose and further decomposition products .....	8
Figure 4: Sulfonation of naphthalene.....	11
Figure 5: Reaction pathways of levoglucosan in water-rich and alcohol-rich mediums ...	15
Figure 6: Sulfonated pine chip char and sulfonated activated carbon .....	18
Figure 7: Bench scale bio-reactor setup.....	22
Figure 8: Fast pyrolysis reactor schematic.....	25
Figure 9: Fast pyrolysis reactor.....	25
Figure 10: ATR analysis in transmittance mode of pine chip char and activated carbon before and after sulfonation .....	29
Figure 11: HPLC chromatograms for 5 g/L xylose standard, products following hydrolysis at 110 °C, 4 hrs., and a thermal control following heating at 110 °C, 10 hours .....	33
Figure 12: Xylose concentration vs. time at various hydrolysis temperatures using birchwood xylan feedstock of 7.3 g/L and sulfonated PCC catalyst .....	34

Figure 13: The effect of rinse method on catalyst activity for hemicellulose hydrolysis at 120 °C using birchwood xylan feedstock of 7.3 g/L sulfonated PCC catalyst .....	34
Figure 14: Reduction in PCC activity as a function of number uses at 120 °C, 2 hrs .....	35
Figure 15: Comparison of PCC and AC activity with xylan at 120 °C .....	37
Figure 16: Comparison of PCC and A15R activity at 90 °C, 110 °C, and 120 °C .....	38
Figure 17: Comparison of PCC and A15R reuse activity with xylan at 120 °C, 2 hrs .....	40
Figure 18: Average rate constant k as a function of change in concentration and time for 90 °C, 110 °C, and 120 °C for an initial xylan concentration of 7.3 g/L, PCC catalyst .....	41
Figure 19: Activation energy $E_a$ of xylose formation as a function of $T^{-1}$ and $\ln(k)$ for initial xylan concentration of 7.3 g/L, PCC catalyst .....	43
Figure 20: Average rate constant k as a function of change in concentration and time for 90 °C, 110 °C, and 120 °C for an initial xylan concentration of 7.3 g/L, A15R catalyst .....	44
Figure 21: Activation energy $E_a$ of xylose formation as a function of $T^{-1}$ and $\ln(k)$ for initial xylan concentration of 7.3 g/L, A15R catalyst .....	45
Figure 22: Reaction rate per gram of PCC as a function of initial xylan concentration at 120 °C .....	46
Figure 23: Effect of agitation rate on reaction rate of PCC xylan hydrolysis at 120 °C....	47
Figure 24: HPLC chromatograms of 10 g/L glucose standard, 1 g/L levoglucosan standard, 17 hr, 123 °C levoglucosan hydrolysis products, and 17 hr, 123 °C levoglucosan thermal control .....	49

Figure 25: Model compound levoglucosan with sulfonated PCC hydrolysis results, 120 °C .....	50
Figure 26: Solid disc formed over the hydrolysis products of ILC aqueous phase bio-oil and PCC catalyst .....	53
Figure 27: HPLC analysis of PCC bio-oil ethanol hydrolysis, 5 hrs, 120 °C .....	55
Figure 28: GC/MS analysis of FP bio-oil before hydrolysis 25 °C , FP bio-oil control 5 hr., FP bio-oil and PCC 5hr. 120 °C .....	56
Figure A.1: Levoglucosan standard curve for HPLC analysis, 5-25 g/L.....	65
Figure A.2: Xylose standard curve for HPLC analysis, 1.25-10 g/L.....	65
Figure A.3: Glucose standard curve for HPLC analysis, 0.5–10 g/L .....	66

## **CHAPTER 1**

### **INTRODUCTION**

Crude oil was once an abundant, inexpensive, liquid fuel source that provided mankind with all of the benefits and opportunities only available to industrialized societies. That resource is now dwindling, and an alternative must be found in order to maintain those benefits and opportunities to which mankind has become so accustomed. Sustainable alternatives, such as biofuels, can be produced from biomass co-products of the agricultural and forestry industries. One ton of dry lignocellulosic biomass is roughly equivalent to 3.15 barrels of oil. As of 2006, the estimated cost of lignocellulosic biomass in the U.S. was significantly lower than the cost of crude oil: \$5 - \$15 per barrel-of-oil-equivalent (boe) versus \$56 per boe respectively (Huber, 2006).

Much like crude oil, biomass must be refined before it can be used as fuel. The term “biorefinery” refers to a sustainable facility comprised of all the processes required to separate and convert biomass into marketable products such as biochemicals and biofuels. The concept of a biorefinery is similar in application to current fossil fuel based refineries. Raw materials are processed and converted into marketable products or feedstocks for the production of further refined products. Utilizing waste materials, or dedicated forest and agricultural biomass eliminates the competition with food and feed industries for feedstock sources. Complex carbohydrates such as hemicellulose and levoglucosan are separated from lignocellulosic material along biochemical and thermochemical platforms. Biorefineries can be integrated into existing industrial

refining systems that produce waste or co-products suitable for biomass feedstock.

Agricultural and forestry are some of the existing industries that involve such materials.

Improving biorefinery production efficiency is imperative for industrial commercialization.

Raw biomass is primarily composed of carbohydrates in the form of cellulose, hemicellulose, and lignin. Cellulose and hemicellulose are complex polymers that can be easily hydrolyzed into fermentable feedstock. Lignin serves as a bonding adhesive, cannot be easily depolymerized, and its monomers are not easily utilized by microorganisms. Therefore, lignin must be separated from cellulose and hemicellulose.

The two main pathways of biomass conversion in a biorefinery are the biochemical and thermochemical platforms shown in figures 1 and 2. One potential biochemical process for a biorefinery is hot-water extraction, hydrolysis of extracts to monomers, the separation of monomers and organic acids, and fermentation of sugars to fuels, chemicals, and other products (Amidon and Liu 2009; Fatih Demirbas 2009; Cherubini 2010). The thermochemical processes of a biorefinery are pyrolysis and gasification, collection of bio-oil and syn-gas, and catalytic conversion of the syn-gas or bio-oil to chemicals and liquid fuels (e.g. esterification of bio-oil) or separation of monomers from organic acids, hydrolysis of complex sugars, and fermentation of monomers (Huber et al. 2006).

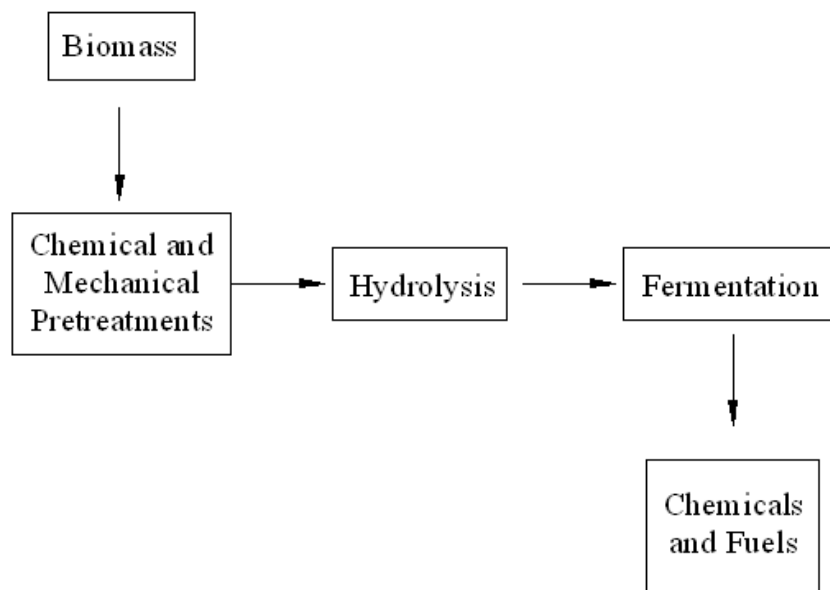


Figure 1. Flow diagram for the biochemical conversion of lignocellulosic biomass to chemicals and fuels

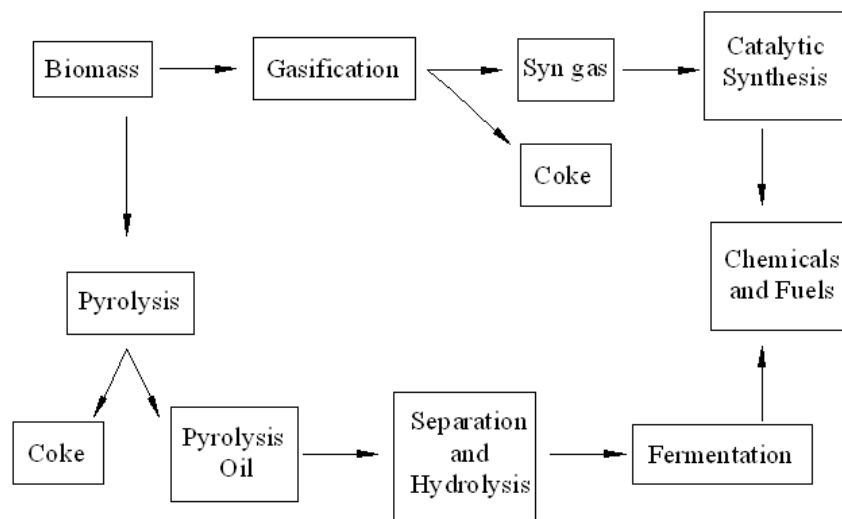


Figure 2. Flow diagram for the thermochemical conversion of lignocellulosic biomass to chemicals and fuels

Biochemical and thermochemical platforms each generate products that can be hydrolyzed to form a fermentable feedstock. Existing hydrolysis methods are expensive and inefficient due to pretreatments required to deconstruct structural lignin and crystalline cellulose, the production of fermentation inhibitors, and expenses associated with enzyme use and production (Huber et al. 2006; Merino and Cherry, 2007). The efficiency of current hydrolysis methods could be improved by using an alternative catalyst. Carbon based solid acid catalysts are more sustainable than existing enzymatic and liquid acid catalysts, which are neither recoverable nor reusable. Furthermore, these solid acid catalysts can be generated within biorefineries from existing co-products for use across both biochemical and thermochemical production platforms.

## **CHAPTER 2**

### **HYPOTHESIS AND OBJECTIVE**

#### **Hypothesis**

1. Biochar generated from biomass such as pyrolyzed pine chips will form a high surface area, porous, carbon based structure.
2. It is theorized that the carbon surface can support functionalized catalytically active acid groups.
3. Functionalized acid groups once bound to the support structure will remain catalytically active allowing recovery and reuse of the solid acid catalyst.
4. It is theorized that the synthesized solid acid carbons will be catalysts for hydrolysis and esterification reactions.
5. The reaction rates and product yield will be comparable to dilute liquid acid catalysts and more favorable than enzymatic catalysts.
6. The catalyst will be suitable for the hydrolysis of hemicellulose to xylose across the biochemical platform and the hydrolysis of levoglucosan to glucose across the thermochemical platform of a biorefinery.

#### **Objective**

The specific objectives of this study can be summarized as

1. To synthesize solid acid catalysts from biochar.
2. To verify the presence of a stable functionalized acid group on the catalyst surface.

3. To measure the physical and chemical characteristics of the solid acid catalyst.
4. To investigate the reaction kinetics of hemicellulose hydrolysis.
  - a. To evaluate the effect of reaction temperature and mass transfer on the hydrolysis reaction.
  - b. To develop a representative rate law for the proposed reactions using model compounds.
5. To quantify the potential for recovery and reusability of the solid acid catalyst.
6. To compare the measured reaction kinetics with commercially available synthetic solid acid catalysts.
  - a. To compare the rate of reaction under common conditions
  - b. To compare the type and quantity of compounds formed.
7. To qualify and quantify the products generated from levoglucosan hydrolysis within fast pyrolysis bio-oil.

## **CHAPTER 3**

### **LITERATURE REVIEW**

#### **Hemicellulose Extraction**

Biomass must first be pretreated to separate lignin from complex sugars that can be hydrolyzed to fermentable monomers. The three primary complex polymers of woody biomass are cellulose, hemicellulose, and lignin. Lignin is an irregular polymer serving as an adhesive holding the other two components together. Cellulose is a crystalline polymer composed primarily of glucose. Hemicellulose is an amorphous polymer composed of five and six carbon sugars including xylose, arabinose, galactose, glucose, and manose (Huber et al. 2006). Liquid hot-water extraction, steam explosion, dilute acid extraction, and alkaline pretreatment are some of the common biochemical pretreatments used to separate the various biomass components. The purpose of these pretreatments is to extract hemicellulose, solubilize the cellulose fibers, and remove the lignin barrier (Huber et al. 2006; Kumar et al. 2009a; Mosier et al. 2005). Hot-water extraction is the most advantageous pretreatment because it is inexpensive, non-toxic, and does not generate compounds that inhibit the downstream fermentation process. Hemicellulose is the most easily separated oligomer during hot-water pretreatment. Unfortunately, the hemicellulose stream cannot be fermented directly. An additional hydrolysis reaction is required to separate the oligomer products into fermentable monomers such as xylose (Mosier et al. 2005). Xylan, the predominant sugar polymer composing hemicellulose, is a renewable resource that is not currently being utilized to

its full potential in the development of fuels, chemicals, and materials (Amidon and Liu, 2007). The reaction pathway for the conversion of xylan to xylose and further decomposition products such as furfural is shown in figure 3.

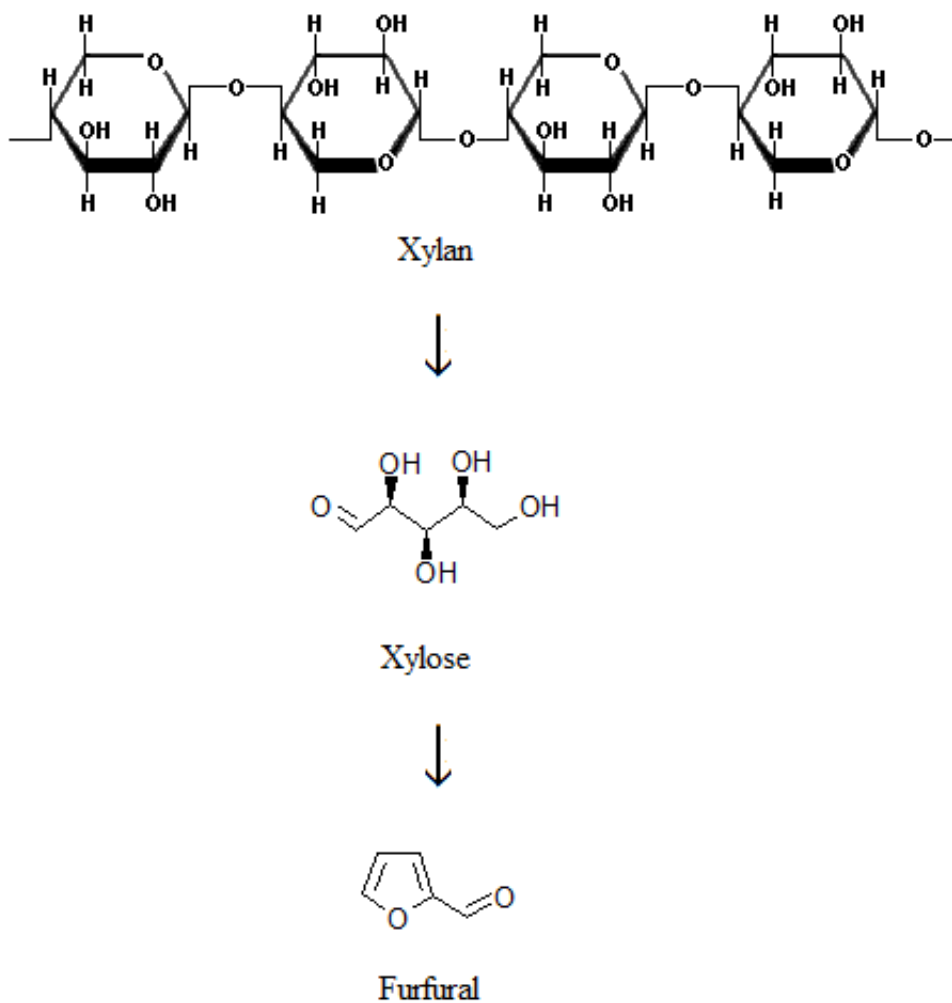


Figure 3. Reaction pathway for the acid hydrolysis of xylan to xylose and further decomposition products.

## **Liquid Acid and Enzymatic Catalysts**

Liquid acid catalysts, such as sulfuric acid, generate over a 90% yield of monomers when hydrolyzing hemicellulose at temperatures of 90 – 100 °C (Jin et al. 2011; Mosier et al. 2005). However, these catalysts are dangerously caustic with the potential to cause burns and damage equipment and produce hazardous waste (Maggi et al. 2008; Mosier et al. 2005; Okuhara 2002). Furthermore, these acids continue to break down monomers such as xylose into furfural that must be removed through distillation. Residual acids inhibit downstream fermentation processes. The required neutralization procedures reduce efficiency and increase production expenses (Huber et al. 2006; Kumar et al. 2009a; Mosier et al. 2005). While enzymatic hydrolysis is safe for both the operator and the environment, the enzymes themselves are expensive, non-recoverable, and have a lower reaction rate than acid catalysts. Required residence time and production yields vary widely between enzymatic catalysts. A hydrolysis reaction of extracted hemicellulose with *Fusarium graminearum* xylanase blend has a maximum xylose yield of approximately 61% after 4 hours at 60 °C while *Thermomonospora fusca* has a maximum yield of 58.6% after 3 hours at 60 °C (Carapito et al. 2008). A 2009 study by the SUNY College of Environmental Science and Forestry of four different xylanase catalysts found maximum yield variations between 28% and 68% with retention times up to 4 days (Amidon and Liu 2009).

## **Solid Acid Catalysts**

Solid acid catalysts are potential reusability with high production yields and low retention times comparable to liquid acid catalysts. Early solid acid catalysts under study were anion exchange resins. While these resins were successful catalysts, they were

expensive and could be unstable at high pH levels (Pasias et al. 2006; Shibasaki-Kitakawa et al. 2007). Research with perfluorinated alkanes and heteropoly acids as catalysts found similar results. In addition to their expense and instability, the non-renewable carbon source of these catalysts created an undesirable environmental impact. The negative results of perfluorinated alkanes and heteropoly acids can be attributed to the support materials silicon oxide and zirconia (Kulkarni et al. 2006; Lopez et al. 2007).

Amberlyst 15 resin (A15R), a commercially available solid acid catalyst, has been shown to selectively hydrolyze hemicellulose in the form of arabinogalactans into monomers such as arabinose and galactose. This catalyst could be applicable for the conversion of hemicellulose to fermentable feedstocks in a commercial scale biorefinery. A15R is a macroreticular resin sulfonic functional groups supported on styrene-divinyl benzene beads. Product yields for both monomers of approximately 50% were reached at temperatures of 90-100 °C with an agitation speed of 600 rpm after 24 hours (Kusema et al. 2010).

A metallic or synthetic plastic matrix is expensive to produce and less sustainable than an activated carbon matrix developed from biochar. Pyrolyzed biomass will form a catalytic support structure that can be functionalized with acids and bases (Dehkhoda et al. 2010). Carbon based solid acid catalysts are potentially reusable and inexpensive compared to synthetic or metallic based solids. Raw biomass can be pyrolyzed to form a given shape or structure required to support the catalyst. This procedure would not require the cost and lab work associated with refining synthetic support structures, and could be incorporated into a biorefinery. Materials such as pine chips and peanut hulls are inexpensive and readily available in the form of agricultural and forestry resins.

## Biochar Supported Solid Acid Catalysts

Biochar, a slow pyrolysis co-product, has an irregular porous framework that can support carboxylic and sulfonic acid groups. Sulfonation of biochar can be performed via concentrated liquid acid or acidic fuming (Dehkhoda et al. 2010). An example of the sulfonation mechanism is shown in figure 4 below, naphthalene has been substituted for the carbon lattice. Liquid concentrated sulfuric acid is added to solid biochar under heat, then cooled and filtered to separate the sulfonated char from excess liquid acid. The solid is then rinsed with distilled water to further remove any excess acid and dried overnight. For acidic fuming the biochar is pretreated with potassium hydroxide to increase porosity and surface area of biochar. The char is then sulfonated via acidic fuming under heat and nitrogen flow. The products are then rinsed with distilled water and filtered to remove excess sulfate ions from the surface before drying overnight (Dehkhoda et al. 2010; Shu et al. 2010).

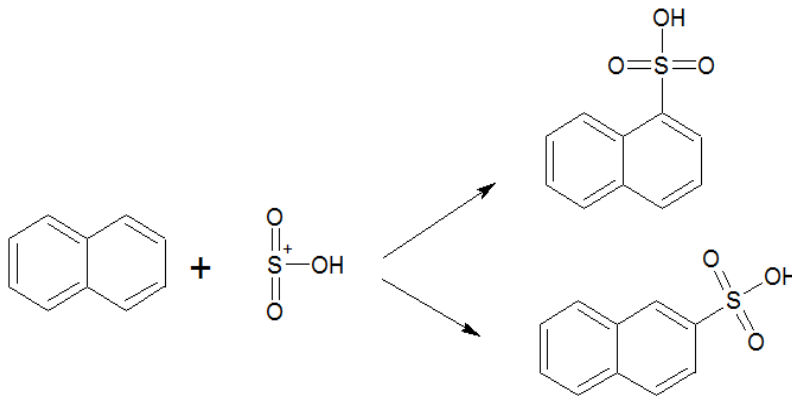
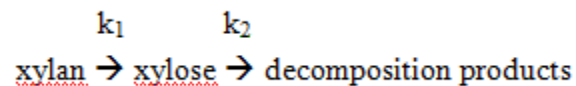


Figure 4. Sulfonation of naphthalene

The acidity of carbon based solid acid catalysts has been shown to be similar to that of solid acids supported on a zirconia structure, which are commonly used in biodiesel production. The acidic characteristics of these catalysts vary between sulfonation methods. Sulfonic acid densities for fuming and liquid sulfonation methods have been reported in the range of 0.935 - 1.09 and 0.585 – 0.650 mmol/g respectively (Dehkhoda et al. 2010). Solid acid catalysts of this type have shown significant activity in the esterification of free fatty acids. Further research is required regarding their potential biorefinery applicability.

### **Hemicellulose Hydrolysis Kinetics**

The hydrolysis mechanism is difficult to model accurately due to the complex structure of hemicellulose. Therefore pseudo-homogeneous kinetic models have often been used to model hemicellulose hydrolysis reactions to xylose with dilute liquid sulfuric acid (Jin et al. 2011). The hemicellulose hydrolysis reaction is assumed to be an irreversible first order reaction or series of first order reactions where  $k_1$  is the reaction rate constant for xylose formation and  $k_2$  is the reaction rate constant for xylose degradation (Lavarack et al. 2000; Jin et al. 2011, Yat et al. 2007).



Following this assumption, the first order rate law equation has the form:

$$-dC_A/dt = -r_A = kC_A$$

$C_A$  represents the concentration of hemicellulose,  $r_A$  represents the reaction rate of hemicellulose hydrolysis to xylose, and  $k$  represents the reaction rate constant.

Activation energies analyzed by an Arrhenius type equation have been reported in a

varied range for the hydrolysis of hemicellulose to xylan depending on the type of feedstock and efficiency of catalyst. Hydrolysis reactions with dilute sulfuric acid and both corn stover and hardwood hemicellulose have similar reported ranges of approximately 130 – 170 kJ/mol (Lu and Mosier 2008; Yat et al. 2007).

### **Levoglucosan Extraction**

Pyrolysis, a thermochemical decomposition process, is a procedure in which biomass is heated in an inert environment and converted into solid, liquid, and gaseous products in the absence of steam or oxygen (Huber et al. 2006). Approximately 61% of the initial biomass is converted to bio-oil, a liquid product of pyrolysis (Boetang et al. 2007). Pyrolysis bio-oil contains high concentrations of a cellulose-derived molecule known as levoglucosan (Helle et al. 2007). Levoglucosan is extracted from the aqueous phase of bio-oil. The initial water content of fast pyrolysis bio-oil is approximately 20% (Bennett et al. 2009). Additional water is added to increase the ratio to 1:1 before fast pyrolysis oil is phase separated through a centrifuge. Depending on the type of lignocellulosic material, existing fast pyrolysis processes have been shown to generate levoglucosan from aqueous phase bio-oil with concentrations ranging from approximately 27 to 120 g/L (Tessini et al. 2011; Bennett et al. 2009). The solid pyrolysis product, charcoal, maintains the original morphology of the lignocellulosic material and could serve as an organic solid catalyst structural platform.

### **Levoglucosan Hydrolysis**

Levoglucosan can be hydrolyzed to form glucose, a fermentable monomer, or esterified to methyl  $\alpha$ -D-glucopyranoside (MGP), an acetal of glucose, depending on the hydrolysis medium. The reaction pathway for the formation of these compounds from

levoglucosan is shown in figure 5. Fast pyrolysis bio-oil can be simultaneously esterified to form esters in an alcohol-rich medium, while levoglucosan is hydrolyzed to glucose with acid-catalysts in a water medium. As temperatures increase above approximately 130 °C glucose and MGP are no longer the primary products. The conversion process continues to generate intermediate dehydrated sugars such as 5-(hydroxymethyl)furfural (HMF) in a water medium or 2-(dimethoxymethyl)-5-(methoxymethyl)furan (DMMF) in an alcohol medium, and finally levulinic acid or methyl levulinate can be formed (Hu and Li, 2011). These final products are marketable compounds in the food, diesel fuel, and fragrance industries. However, in a water rich medium, glucose is easily polymerized into solid humins that diminish the total yield glucose or levulinic acid. Solid acid catalysts combined with esterification agents can be used to stabilize fast pyrolysis oil and reduce polymerization of glucose. Nearly 100% conversion of levoglucosan can be achieved after 1 hour for temperatures greater than 110 °C (Hu and Li, 2011). The Fuels and Energy Technology Institute of Curtin university in Perth, Australia has demonstrated the simultaneous hydrolysis and esterification of fast pyrolysis bio-oil with a solid acid catalyst and methanol over a thermal range of 70 – 170 °C. Levoglucosan hydrolysis to glucose became significant at temperatures above 90 °C and the reaction rate increased proportionally with the temperature of the reaction (Gunawan et al. 2011).

Liquid acid hydrolysis of fast pyrolysis bio-oil at temperatures above 120 °C has been shown to generate glucose yields greater than 100%. According to a 2003 study by the Chinese Academy of Sciences, this generation of excess glucose can be attributed to the hydrolysis of intermediate cellulose oligomers such as cellobiosan (Yu and Zhang, 2003). Hydrolysis of levoglucosan in bio-oil with a liquid acid poses similar problems to

those found in the hydrolysis of hemi-cellulose. Compounds such as furfural, hydroxymethyl furfural, and organic acids generated during the liquid acid hydrolysis reaction inhibit downstream fermentation (Bennett et al. 2009).

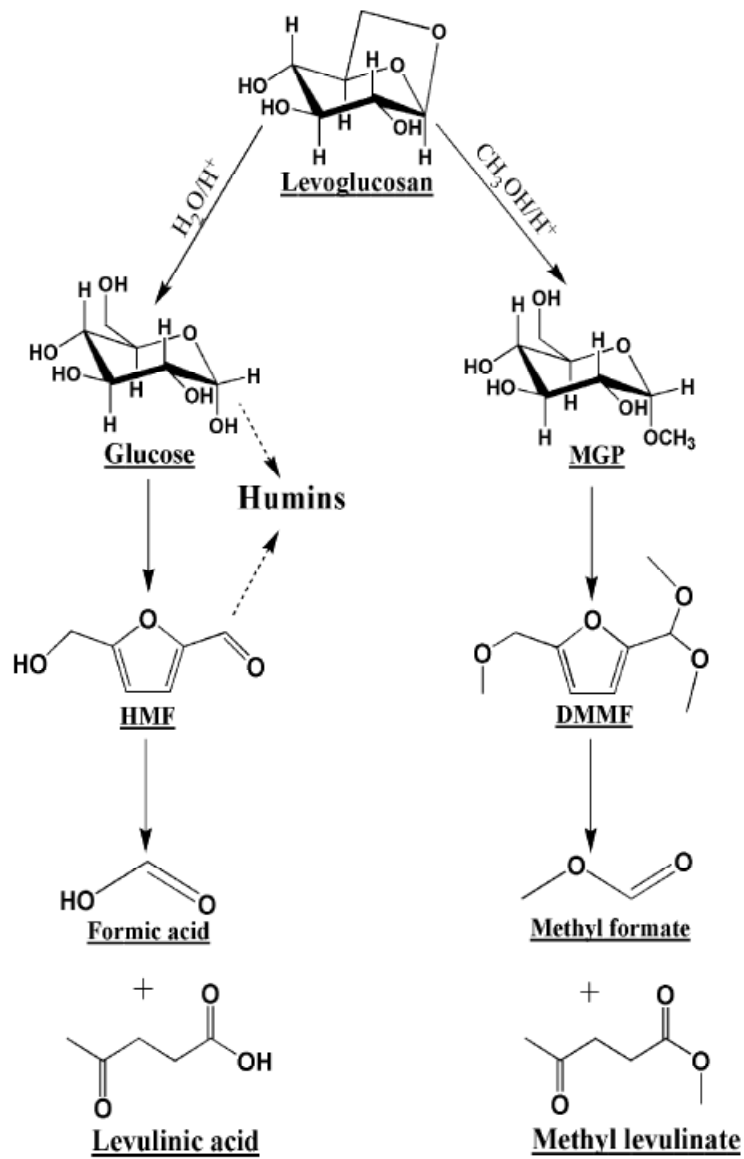


Figure 5. Reaction pathways of levoglucosan in water-rich and alcohol-rich mediums (Hu and Li, 2011).

## **CHAPTER 4**

### **MATERIALS AND METHODS**

#### **Model Compounds**

Birchwood xylan (Sigma-Aldrich, St. Louis, MO) was selected to represent a hardwood hemicellulose due to its high purity of xylose. Birchwood xylan has a reported degree of polymerization of approximately 70 for xylose (Teleman, Larsson, and Iversen, 2001). This xylan model compound was used for all hemicellulose experimentation. The model compound, levoglucosan (Carbosynth, Berkshire, UK), was used for preliminary hydrolysis experimentation before proceeding to levoglucosan rich fast pyrolysis oil.

#### **Biochar Synthesis and Sulfonation**

Locally purchased pine chips (Southern Pine) were pyrolyzed at in a slow pyrolysis batch reactor (316SS, 23 x 23 x 23 cm reactor, with a N<sub>2</sub> purge line and exhaust) inside of a furnace (Thermolyne, Barnstead Inc, La; Thermolyne single set point, 1200°C max, 10°C/min ramp). Pyrolyzed chips were ground to a particle size range of 1.6 - 4.8 mm. Initial biomass samples of 2-5 g. were retained in the reactor for 1 hour at 400 °C with a pure nitrogen sweep gas flowing at 1-2 L/min to generate biochar. Ten grams of biochar chips were soaked in concentrated sulfuric acid with an acid to char ratio of 2 mL to 1 g. The sulfonated pine chip char (PCC) char was dried overnight at 100 °C and then rinsed with de-ionized water at room temperature until the pH of the rinsate stabilized and dried again overnight at 100 °C. Following the first round of preliminary experimentation, ion chromatography analysis revealed that inadequate

rinsing procedures left unbound acids within the catalyst that could influence the hydrolysis reaction. The rinse procedure was modified to thoroughly remove this excess acid. The PC char was divided into sub-samples, each weighing approximately 13 g (wet). Each batch was pre-rinsed with 100 mL of DI water for 10 minutes at room temperature. Then each sample was rinsed with 1 L of DI water for 1 hour at 80 °C, followed by a 15 minute rinse at room temperature. An aliquot of rinsate was saved for IC analysis. The warm rinse procedure was repeated until the rinsate sulfate concentration was < 5ppm, which was achieved after 3 warm rinses. The char was dried overnight at 100 °C.

### **Activated Carbon Sulfonation**

Mead Westvaco Nuchar WV-B-20 activated carbon was also used as a support structure for a carbon based solid acid catalyst. The Nuchar WV-B-20 has a particle size of 6 x 18 ((US Mesh, 8% oversize, 5% undersize) and an apparent density of 240-300 kg/m<sup>3</sup>. Ten grams of WV-B-20 were sulfonated with 13 mL concentrated H<sub>2</sub>SO<sub>4</sub>. The sulfonated activated carbon (AC) was dried overnight at 100 °C. The AC char was divided into three samples, each weighing approximately 11.3 g (wet). Each batch was pre-rinsed with 100 mL of DI water for 10 minutes. Then each sample was rinsed with 1 L of DI water for 1 hour at 80 °C, followed by a 15 minute rinse at room temperature. IC analysis showed a sulfate ion concentration less than 1 ppm following the second rinse. The char was dried overnight at 100 °C. An image of the AC and PCC catalysts is shown in figure 6.

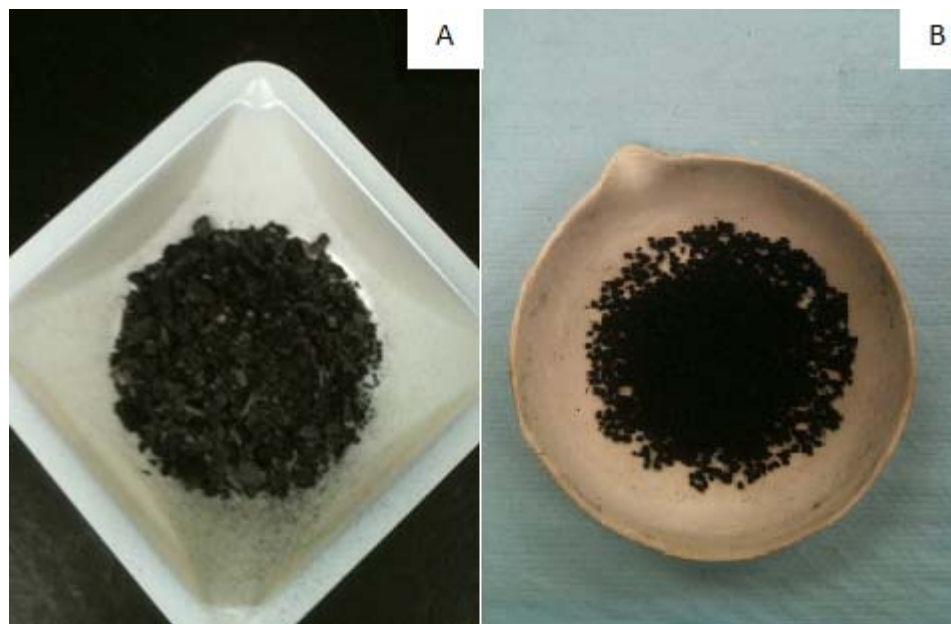


Figure 6. Sulfonated pine chip char (A), and sulfonated activated carbon (B).

### **Analytical Methods**

Catalyst sulfonation was verified using attenuated total reflectance (ATR) and CHNS analysis. An unsulfonated pine chip char sample was compared against a sulfonated sample for ATR analysis. All samples were ground to a fine powder before analysis via Grazing Angle Attenuated Total Reflection Fourier Transform Infrared Spectroscopy (GATR-FTIR). Functional groups on the catalyst surface were isolated by using an ATR incident angle with a limited depth of penetration (~150 nm). CHNS analysis was used to verify the retention of sulfonic groups to the surface of the catalyst following multiple hydrolysis reactions.

A Dionex ICS-2000 with a Dionex IonPac AS18 column (4 x 250 mm) and 23 mM KOH eluent was used for ion chromatogram analysis to determine the presence and concentration of unbound sulfate groups in catalyst rinsate. Samples were injected on the column with an auto-sampler at a volume of 20  $\mu$ L sample size. IC retention times were approximately 23 minutes with a flow rate of 1 mL/min and temperature of 30  $^{\circ}$ C.

Standard curves were developed using a Dionex seven anion standard II (sodium sulfate 5, 10, and 20 ppm).

Thermal stability of chars and solid acid catalysts was determined through thermal gravimetric analysis (TGA) with a Mettler-Toledo 851e Thermogravimetric Analyzer. Samples of 10-15 mg were heated from room temperature to 900 °C at a rate of 10 °C/min with a helium carrier gas flowing at 50 ml/min. Loss of mass was recorded against time and temperature. The TGA analysis was used to verify that the sulfonation procedure did not reduce the thermal stability of the chars and to determine the conditions for temperature program desorption studies.

Acid density analysis was performed with an acid-base titration using 0.1 N NaOH and 1 N HCl. Three types of each AC and PC char were selected: unsulfonated (clean) char, sulfonated char, and sulfonated char following a hydrolysis reaction (after 1<sup>st</sup> use). A 0.1 N NaOH solution was prepared to soak the char at a ratio of 150 mL to 1 g. The char/base solution flasks, along with a single “blank” flask (control base solution), were mixed on a room temperature shaker table overnight at 145 rpm. The samples were filtered for HCl titration. The molarity of the 1.0 N HCl was verified along with the molarity of the 0.1 N NaOH blank. The volume of acid required to neutralize the excess base of each sample was recorded. The acid density of each catalyst sample was calculated from these values using the following equations:

$$M_{\text{HCl}}V_{\text{HCl}} / V_{\text{NaOH}} = M_{\text{NaOH}}$$

$$(M_{\text{NaOH}0} - M_{\text{NaOH}}) V_{\text{NaOH}} / W_{\text{catalyst}} = \text{Total acid density}$$

The molarity and volume of HCl consumed are represented by  $M_{\text{HCl}}$  and  $V_{\text{HCl}}$  respectively. The molarity and volume of NaOH after neutralizing all acid available on the catalyst are represented by  $M_{\text{NaOH}}$  and  $V_{\text{NaOH}}$  respectively.  $M_{\text{NaOH}0}$  represents the starting molarity of the base solution used to neutralize the catalyst.  $W_{\text{catalyst}}$  is the weight of the catalyst reacted with the NaOH solution.

Catalyst surface area and pore size were determined through BET surface analysis (BET theory is named for its inventors S. Brunauer, P. H. Emmett, and E. Teller). Char samples of approximately 0.150-0.180 g were analyzed through a Quantachrome autosorb via automated  $\text{N}_2$  adsorption over a relative pressure range ( $P/P_0$ ) of 0.05 to 0.35 using a 7-point BET analysis equation (Quantachrome AUTOSORB-1C; Boynton Beach, Florida).  $P$  represents the pressure at equilibrium and  $P_0$  represents the saturation pressure. BJH analysis  $\text{N}_2$  desorption curves were used to estimate the pore size distribution, average pore radius, and total pore volume of the catalysts. All samples were degassed ranging from 100 to 150 °C for 3 to 4 hours before analysis.

High Performance Liquid Chromatography (HPLC) analysis was used to measure the concentrations of hydrolysis products and reactants (when possible). A Shimadzu LC-20AT liquid chromatogram with a 300 x 7.5 mm Transgenomic Coregel 64H column at approximately 700 - 1000 psi and 60 °C with a 4 mN sulfuric acid eluent flowing at 0.6 mL/min was used to analyze 5  $\mu\text{L}$  samples from levoglucosan and hardwood hemicellulose hydrolysis. Standard curves for xylose, glucose, and levoglucosan were developed using model compounds. Any products with a concentration range outside of the standard curve were diluted to fit within the curve. Liquid samples were diluted when necessary and filtered through a 0.45  $\mu\text{m}$  Millex

syringe filter for HPLC analysis. Standardized retention times were used to identify compounds and standardized peak area to concentration ratios were used to calculate concentration.

### **Hemicellulose Hydrolysis**

The bench scale reactor was composed of a RT-elite stainless steel top stirring hot plate, ACE glass 26 mm aluminum well plate, and 20 mL ACE glass #15 pressure tubes. Solutions of model Birchwood Xylan (Sigma-Aldrich) and de-ionized water were added to individual reactor tubes in various concentrations with a ratio of 10 mL solution to 1 g of PC catalyst. A thermal control was used to verify that hydrolysis did not occur without catalyst. The hydrolysis temperature range included 90, 110 and 120 °C. Agitation rates within the reactors included 250, 500 and 650 rpm. Individual pressure tubes were removed for analysis at regular intervals ranging from 15 minutes to 24 hours at each temperature profile. Temperature values for the tubes were measured in a dedicated reactor with an OMEGA thermocouple submerged in an ACE glass thermo-well fitted for the pressure tube. The reaction reached thermal equilibrium in 15 - 25 minutes depending on the temperature of the reaction. The reactors were removed at given time intervals and cooled at room temperature. Samples were vacuum filtered through a 0.45 um Whatman filter and sub-sampled for HPLC analysis. Sub-samples were diluted and re-filtered through a 0.45 um Millex nylon syringe filter. All liquid samples were stored at 4 °C. The catalyst was dried at room temperature and stored for re-use. The bench scale bio-reactor setup is shown in figure 7.

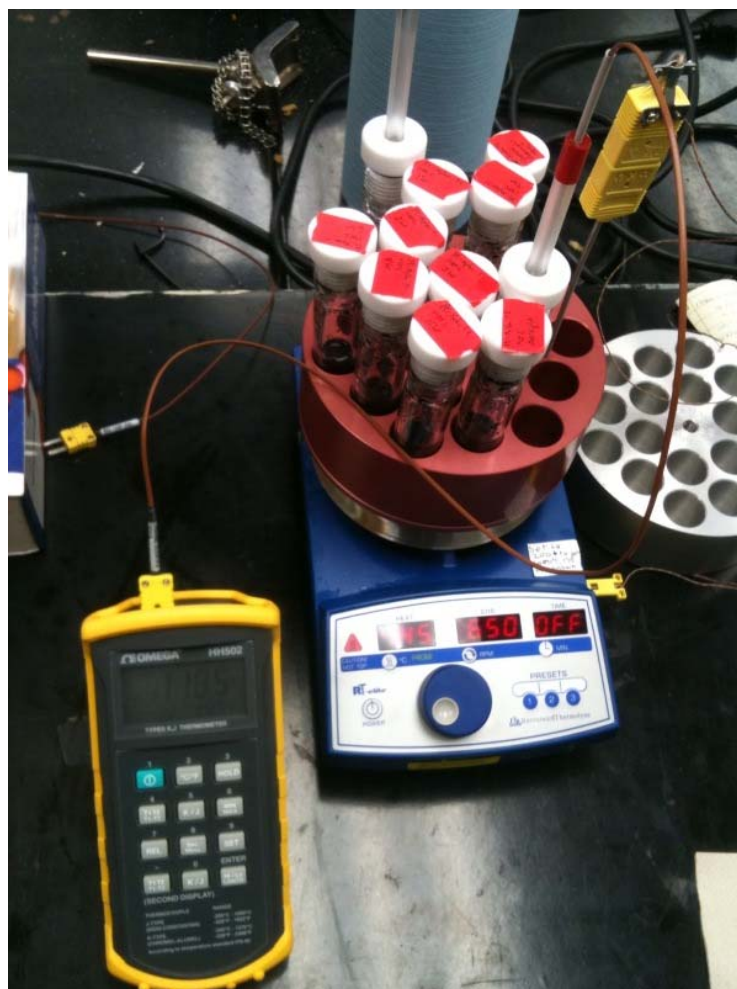


Figure 7. Bench scale bio-reactor setup.

Used solid acid catalyst samples were re-used under the same hydrolysis conditions as the primary reaction. Reuse reactions had a retention time and temperature of 2 hours and 120 °C (these values were selected from the maximum product yield determined by HPLC analysis of the primary reactions). All reactions were performed in duplicate following the sample, filter, and storage procedures of the primary reactions. Solid acid catalysts were collected and reused for three additional reactions following the primary reaction.

The xylose content within the model hemicellulose compound (birchwood xylan) was determined by NREL methods (Sluiter et al., 2008). Xylan concentrations of 10, 25, 35, and 50 g/L were mixed in a 4% sulfuric acid solution. Ten mL samples of this solution were heated for 1 hour at 120 °C. Xylose sugar recovery standards were prepared under the same conditions to correct for further decomposition due to the dilute acid hydrolysis. Xylose product yield was measured via HPLC analysis. The average xylose concentration for birchwood xylan was approximately 73% by mass.

### **Amberlyst 15 Resin**

Amberlyst 15 resin (Sigma-Aldrich), a commercially available solid acid catalyst, was used as a benchmark for hemicellulose hydrolysis. A15R is a styrene-divinylbenzene macroreticular resin with sulfonic acid functional groups. The average particle size for A15R is 0.45-0.60 mm with pore sizes of 40-90 nm (Kusema et al. 2010). The thermal stability limit reported by the manufacturer for A15R is 120 °C. A15R was purchased with an approximate moisture content of 48%. Hemicellulose hydrolysis reactions were carried out under the same conditions as PCC and AC catalysts.

### **Hemicellulose Hydrolysis Kinetics**

The hemicellulose hydrolysis reaction was assumed to be an irreversible first order reaction or series of first order reactions with a rate law equation of the form:

$$-dC_A/dt = -r_A = kC_A$$

The concentration of xylan at a given time  $t$  is described as  $C_A$  and the rate of change in this concentration is described as  $r_A$ . The rate constant  $k$  can be calculated from the production results of a series of hydrolysis reactions with various xylan concentrations. The rate constant  $k$  is also defined by the Arrhenius equation:

$$k=Ae^{-E_a/RT}$$

In this form  $E_a$  represents the activation energy in terms of kJ/mol.  $R$  is the universal gas constant and  $T$  is the temperature of the reaction in Kelvin. The pre-exponential factor  $A$  is also known as the frequency factor with units of  $s^{-1}$ . The Arrhenius equation can be rewritten as:

$$\ln(k) = -E_a R^{-1} T^{-1} + \ln(A)$$

The activation energy can be solved after determining the slope of the linear relationship between  $\ln(k)$  as a function of  $T^{-1}$ .

### **Fast Pyrolysis Oil**

Two forms of fast pyrolysis oil production were used to generate the levoglucosan feedstock: ground pine chip fast pyrolysis (FP) and ground pine pellet in-line-condensation fast pyrolysis (ILC). HPLC analysis was performed on bio-oil samples diluted to 5% with de-ionized water to identify and quantify the initial compounds found in the oil. Both forms of pyrolysis occurred under bubbling fluidized bed conditions. A schematic of the pyrolysis reactor is shown in figure 8 and an image of the actual reactor is shown in figure 9. The pyrolysis reactor utilized a nitrogen sweep gas with a pyrolysis reactor gas flow rate of 20 L/min with 16-18 L/min of fluidization. The residence time of any solids was approximately 5s at reaction temperatures of 500 °C. The oil feed rate to the reactive condensation unit was 40-147 g/hr. The ILC bio-oil generation had an additional process that added water vapor at to the oil condenser.

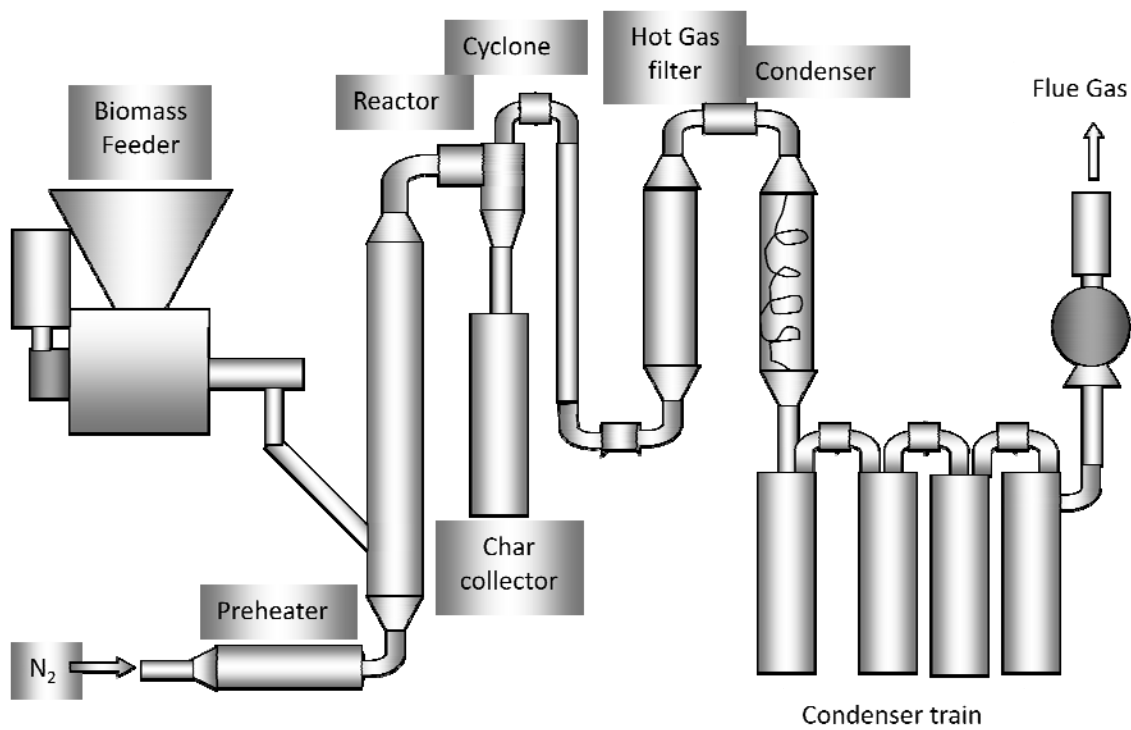


Figure 8. Fast pyrolysis reactor schematic

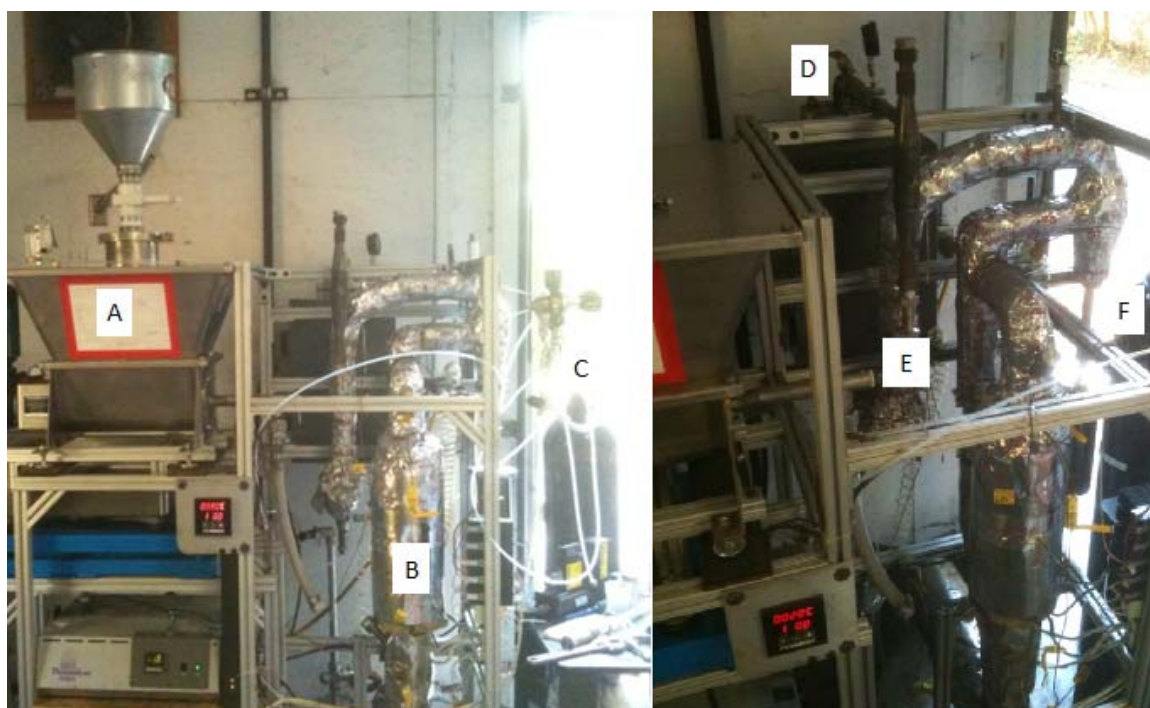


Figure 9. Fast pyrolysis reactor: biomass hopper (A), sand bed reactor (B), nitrogen sweep gas (C), hot gas filter (D), condenser inlet (E), and char collector (F).

The water spray rate of the ILC method was 79-102 g/hr via a small bore atomizer. The final oil product of the ILC method was a 50/50 wt. mix of water and oil, which allowed extraction of the aqueous phase bio-oil directly from the reactor. All pyrolysis procedures were designed and carried out by Roger Hilton, Research Engineer II at the Driftmier Engineering Center at the University of Georgia.

### **Levoglucosan Hydrolysis**

Catalyst activity with model levoglucosan (Carbosynth, Berkshire, UK) was verified using the same materials and methods as model hemicellulose with minor changes in levoglucosan concentration and catalyst ratios.

ILC bio-oil samples had an approximate water/oil ratio of 50%, and had not been filtered before the hydrolysis reaction. Ten mL of the ILC oil was combined with 1 g of catalyst and heated to 120 °C over time intervals ranging from 1 to 24 hours. A 10 mL sample of ILC oil was prepared without the catalyst as a thermal control. Hydrolysis products were gravity filtered through a coarse glass fiber Whatman filter then diluted to 10% with de-ionized water and re-filtered for HPLC analysis.

### **Simultaneous Esterification and Hydrolysis**

Fast-pyrolysis bio-oil samples were vacuum filtered through a 0.45 µm glass filter before characteristic analysis. Ethanol was mixed with the samples at a 1:1 ratio to catalytically esterify the acids and aldehydes within the bio-oil while levoglucosan was simultaneously hydrolyzed to glucose with an expected 1:1 molar ratio. Ten mL of the ethanol/bio-oil mixture was combined with 0.25 g of each solid acid catalyst (sulfonated pine chip char and sulfonated activated carbon). Two controls were prepared: a 10 mL mixture of ethanol/bio-oil without solid acid catalyst and a mixture of 5 mL bio-oil with

0.25 g of solid acid catalyst. The experimental samples and controls were heated to 120 °C and agitated at 650 rpm for 5 hours. Separate samples taken before and after the hydrolysis reaction were vacuum-filtered and diluted to 10% with DI water for HPLC analysis.

## CHAPTER 5

### HEMICELLULOSE RESULTS AND DISCUSSION

#### Catalyst Characterization

The presence of a sulfonic group on the surface of each catalyst was verified with ATR and CHNS analysis. ATR analysis revealed a peak located at 1035-1200  $\text{cm}^{-1}$ , range, which suggests successful sulfonation. Peaks at 1037, 1040, and 1200  $\text{cm}^{-1}$  are indicative of S=O and  $-\text{SO}_3$  groups (Xu et al., 2008). Figure 10 shows these peaks in the sulfonated samples and their absence in the control for both PCC and AC chars.

No sulfur was detected in the untreated biochar, therefore the sulfur composition measured by CHNS analysis is assumed to be due to the presence of the  $\text{SO}_3^-$  group bound to the surface of the catalyst. The sulfur composition following each catalyst use is shown in table 1. Sulfur compounds leached out of the solid acid catalyst following multiple hydrolysis reactions, which rendered the catalyst ineffective after three uses.

Table 1. Sulfonated PCC sulfur composition (CHNS analysis)

Number of Uses	AVG % Sulfur	Std. Dev.
1	1.377	0.027
2	1.293	0.057
3	1.044	0.026
4	0.867	0.066

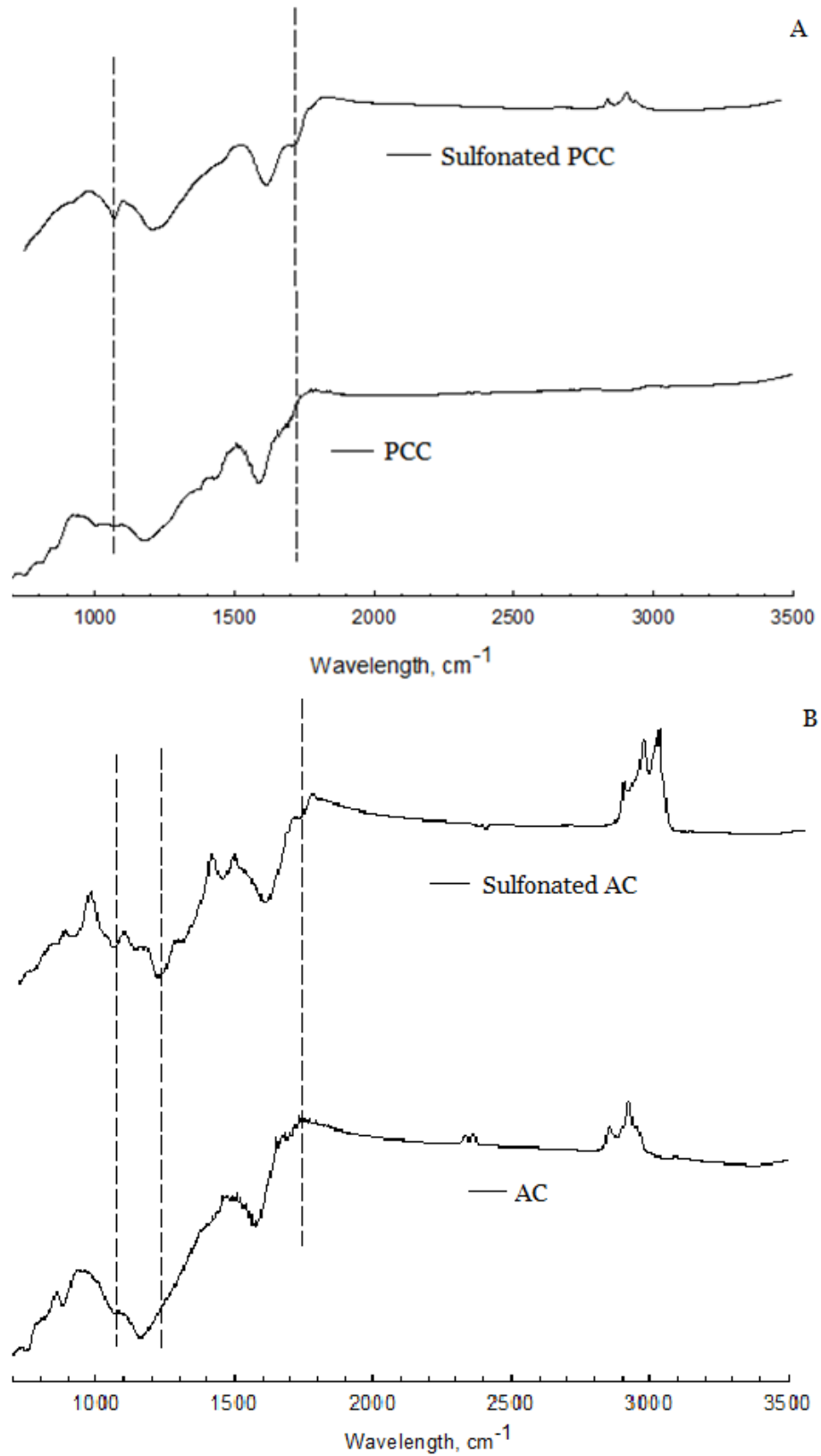


Figure 10. ATR analysis in transmittance mode of pine chip char (A), and activated carbon (B) before and after sulfonation.  $\text{SO}_3^-$  groups peaks appear at  $1040 \text{ cm}^{-1}$ .

The total acid density of the unsulfonated char was subtracted from the total acid density of the sulfonated and used samples to account for any existing organic acids present on the starting material. The total acid density values shown for sulfonated and single use catalysts in table 2 are the acid densities due to sulfonation alone. Sulfonated pine chips had a significantly higher total acid density than sulfonated activated carbon, 3.662 and 0.772 mmol/g respectively. Total acid density was reduced in both groups following a hydrolysis reaction.

The  $\text{SO}_3\text{H}$  acid density was calculated from the sulfur content measured by CHNS analysis using the equation below assuming a one to one molar ratio between sulfur and  $\text{SO}_3\text{H}$ .  $\text{MW}_\text{S}$  represents the molecular weight of sulfur and %S represents the percent sulfur content of the catalyst ( $\text{g}_\text{S}$  per  $100\text{g}_{\text{catalyst}}$ ).

$$\text{SO}_3\text{H acid density} = \%S / \text{MW}_\text{S}$$

The total acid density from acid/base titration was significantly higher than the values suggested by sulfur content measured by CHNS analysis. This discrepancy suggests that the sulfuric acid sulfonation method created additional weak acid groups such as carboxylic acid. Peaks forming at  $1750\text{ cm}^{-1}$  in figure 10 (ATR analysis) confirm the presence of carboxylic acid (Xu et al., 2008).

The surface area and pore size for sulfonated pine chip char samples before and after hydrolysis reactions are shown in table 2. The surface area remains relatively constant with a slight decline from  $365$  to  $308\text{ m}^2/\text{g}$  between initial sulfonation and the second hydrolysis reaction. Surface area was significantly reduced to a range  $< 100\text{ m}^2/\text{g}$  following the third hydrolysis reaction.

Table 2. Physical characteristics of biochar and catalysts

Biochar/Catalysts	Surface Area (m <sup>2</sup> /g)	Pore Volume (cm <sup>3</sup> /g)	Pore Radius (Å)	SO <sub>3</sub> H Acid Density (mmol/g) <sup>a</sup>	Total Acid Density (mmol/g)
PCC - unsulfonated	BD	BD	BD	0.00	0.41
PCC	365	0.1918	10.5	0.69	3.66
PCC - X1	316	0.1657	10.5	0.43	3.05
PCC - X2	308	0.1613	10.5	0.40	NM
PCC - X3	99.1	0.0303	6.1	0.33	NM
PCC - X4	5.3	0.0038	14.3	0.27	NM
AC - unsulfonated	1944	1.2	12.2	0.00	0.20
AC	1391	0.76	11.0	0.20	0.77
AC - X1	NM	NM	NM	NM	0.72

BD – Below detection

NM – Not measured

PCC- X1 – Sulfonated pine chip char after 1 use

AC – X1 – sulfonated activated carbon after 1 use

<sup>a</sup>, Values calculated from % Sulfur composition assuming all sulfur atoms are in the –SO<sub>3</sub>H form with baseline values subtracted.

## **Hemicellulose Hydrolysis with PCC Catalyst**

HPLC chromatograms were used to determine the concentration of xylose following hardwood hemicellulose hydrolysis. The xylose peak was identified given the retention time of a 5 g/L xylose standard. A thermal control was used to verify that hydrolysis did not occur due to heat alone. Figure 11 shows the matching retention times (approximately 11.5 minutes) between the xylose standard (A) and the product of hardwood hemicellulose hydrolysis (B) as well as the absence of xylose in the thermal control (C).

The xylose product concentration as a function of time and temperature is shown in figure 12. A maximum xylose yield of approximately 6.8 g/L, approximately 93% conversion, was achieved from hydrolyzing 7.3 g/L Birchwood Xylan with sulfonated pine chip biochar at 120 °C for 2 hours. Residence times increased to 4 hours to reach a maximum yield of approximately 6.0 g/L at 110 °C. Maximum product yield at a temperature of 93 °C was less than 3.0 g/L after a residence time of 10 hours. The maximum yield residence times and temperatures were used in the catalyst reuse trials.

Once the catalyst preparation procedure had been modified to remove all excess sulfate groups through an 80 °C tri-rinse, the initial hemicellulose hydrolysis reactions were repeated. Figure 13 shows a comparison of the average product concentration over time at 120 °C between the original and modified catalyst rinse methods. The overall trend is maintained between both rinse methods. The difference between the two curves can be attributed to the excess acid remaining in the catalyst following the original rinse procedure. The maximum yield of the modified rinse method has been reduced to 6.4 g/L (approximately 88% conversion), but this yield is due to catalyst activity alone.

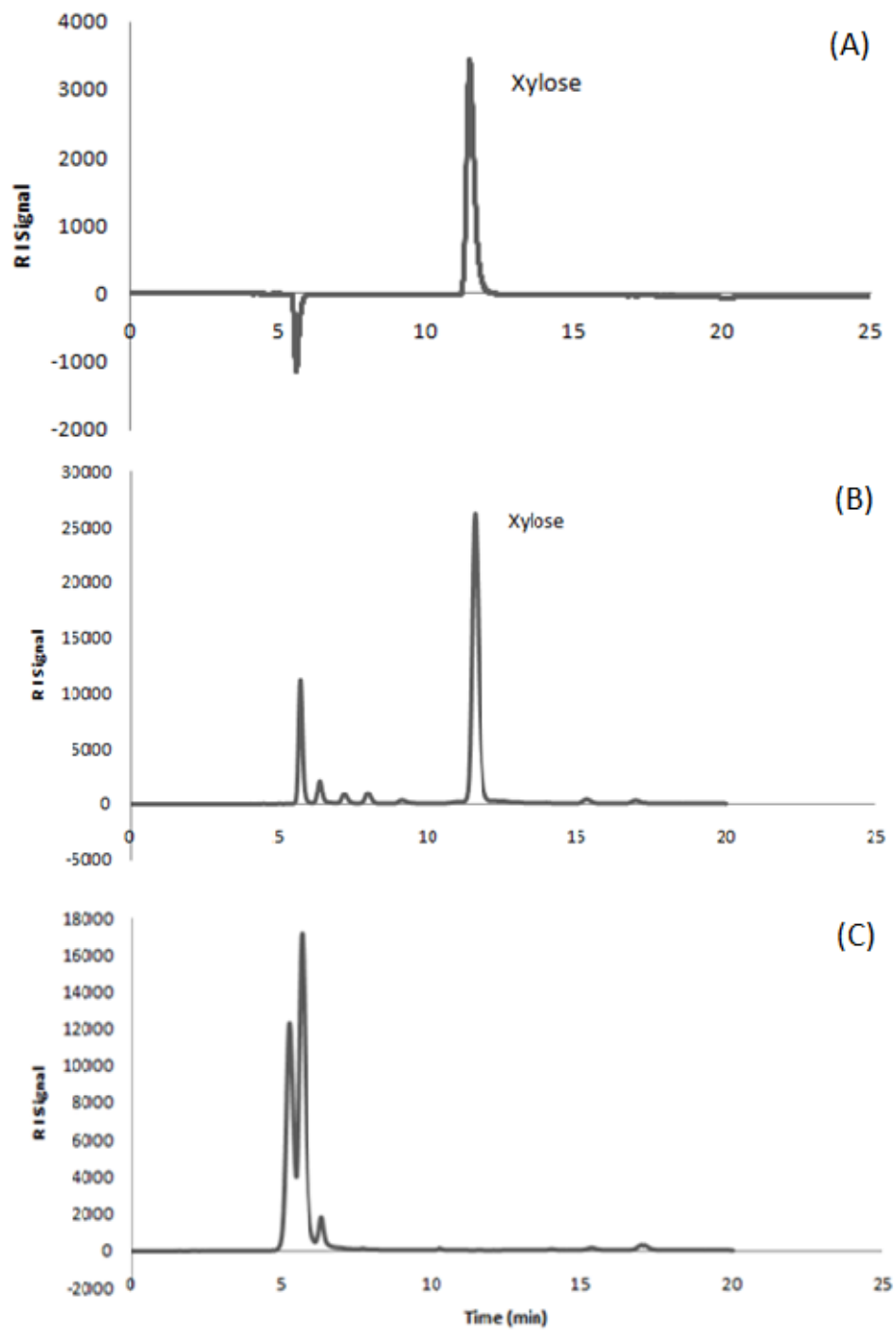


Figure 11. HPLC chromatograms for 5 g/L xylose standard (A), products following hydrolysis at 110 °C, 4 hrs., 650 rpm (B), and a thermal control following heating at 110 °C, 10 hours, 650 rpm (C).

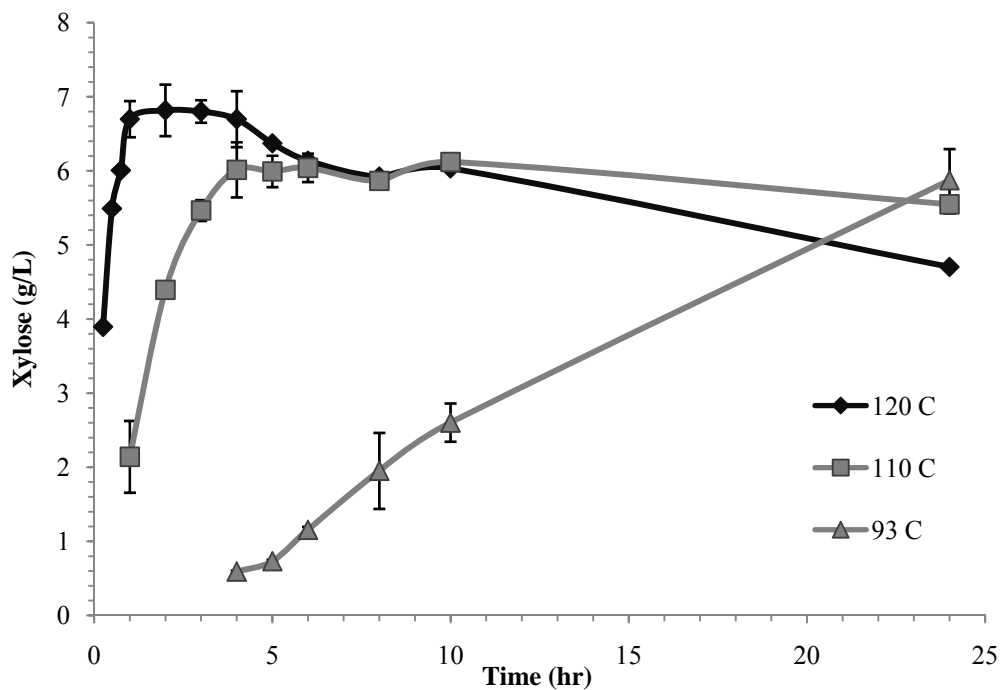


Figure 12. Xylose concentration versus time at various hydrolysis temperatures using birchwood xylan feedstock of 7.3 g/L and sulfonated PCC catalyst (9% wt.), 650 rpm.

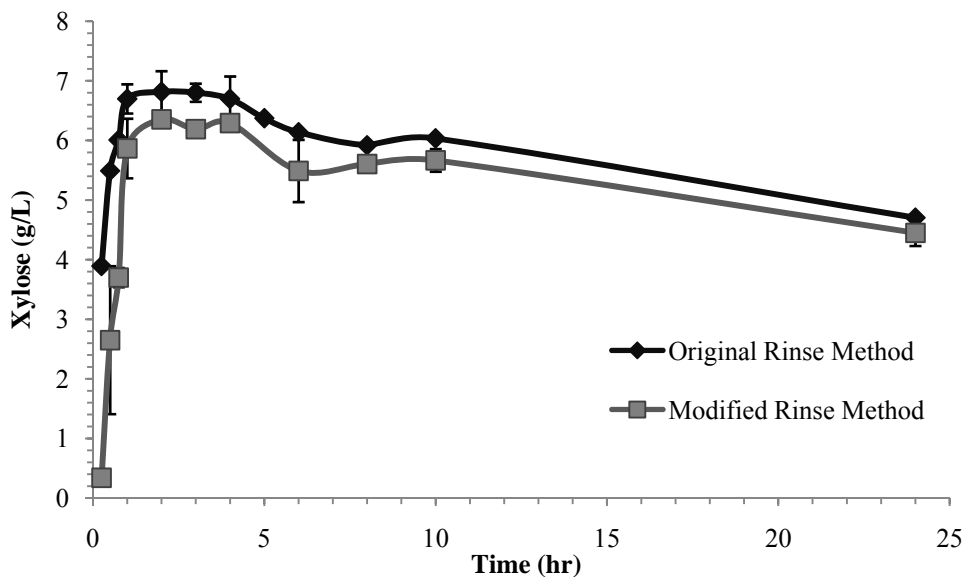


Figure 13. The effect of rinse method on catalyst activity for hemicellulose hydrolysis at 120 °C using birchwood xylan feedstock of 7.3 g/L sulfonated PCC catalyst (9% wt.), 650 rpm.

## Reuse PCC Hemicellulose Hydrolysis

All PCC hemicellulose hydrolysis reuse reactions were performed under the maximum yield conditions of 120 °C, 2 hr., and 650 rpm. Catalyst activity declined significantly with each reuse reaction until the catalyst was rendered inactive by the fourth hydrolysis reaction as shown in figure 14. The activity of the catalyst was reduced almost by half by the second hydrolysis reaction (first reuse). Minimal activity was recorded for the third hydrolysis reaction. The products of the fourth hydrolysis reaction appeared almost identical to the original thermal control and could not be filtered for HPLC analysis.

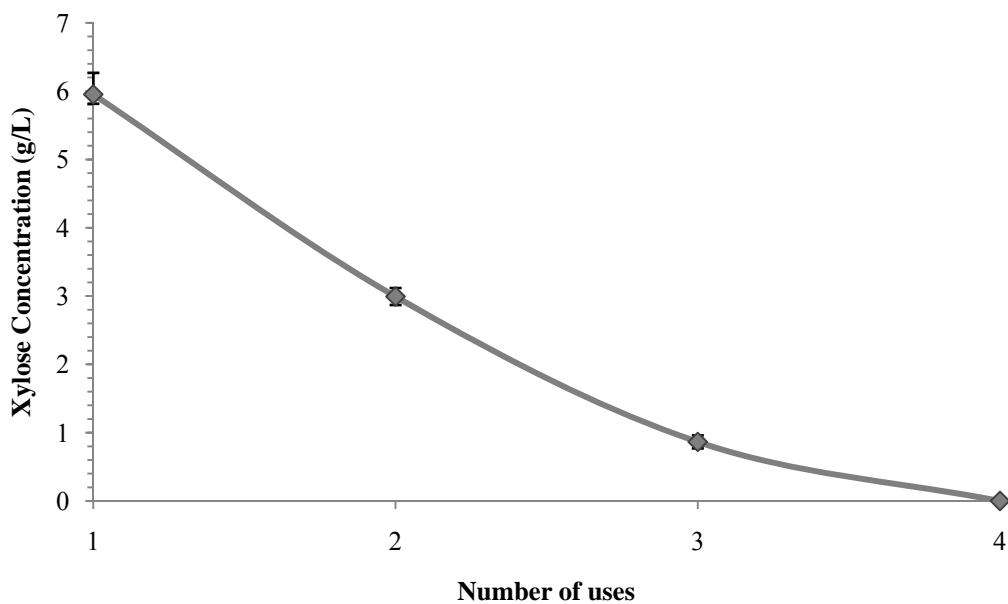


Figure 14. Reduction in PCC activity as a function of number uses at 120 °C, 2 hrs, 7.5 g/L xylan, PCC catalyst (9% wt.) 650 rpm.

The particle size of the PCC catalyst was significantly reduced following the primary hydrolysis reaction. By the end of the second use all of the catalyst had been reduced to a fine powder, some of which passed through the glass fiber 0.45  $\mu\text{m}$  vacuum filter. The decline in activity over multiple uses is most likely due to the quality of the support structure and strong acid site leaching. Declining catalyst activity parallels a decline in physical characteristics such as sulfur content, surface area, pore radius, and total pore volume as shown in tables 1 and 2. These results are probably due to the attrition of the char and acid site leaching resulting from the magnetic stir bar and agitation in the confined area of the tubular reactors. Some portion of the functionalized carbon may also have been lost to fine particles which passed through the glass fiber vacuum filter during catalyst/product separation.

#### **Hemicellulose Hydrolysis with AC Catalyst**

It was theorized that the commercially available activated carbon, which was denser than the pine chip char, may suffer less attrition following multiple hydrolysis reactions. Hemicellulose hydrolysis reactions with the sulfonated activated carbon catalyst were carried out under the maximum yield temperature of 120  $^{\circ}\text{C}$  determined by the PCC hydrolysis trials. A comparison between AC and PCC catalyst activity is shown in figure 15. The AC catalyst showed significantly less catalytic activity than the PCC under the same conditions. Furthermore, the AC showed similar signs of attrition as the catalyst was reduced to a fine powder following the primary hydrolysis reaction. Given the extensive reaction time required to reach a maximum yield with the AC catalyst, no reuse trials were investigated.

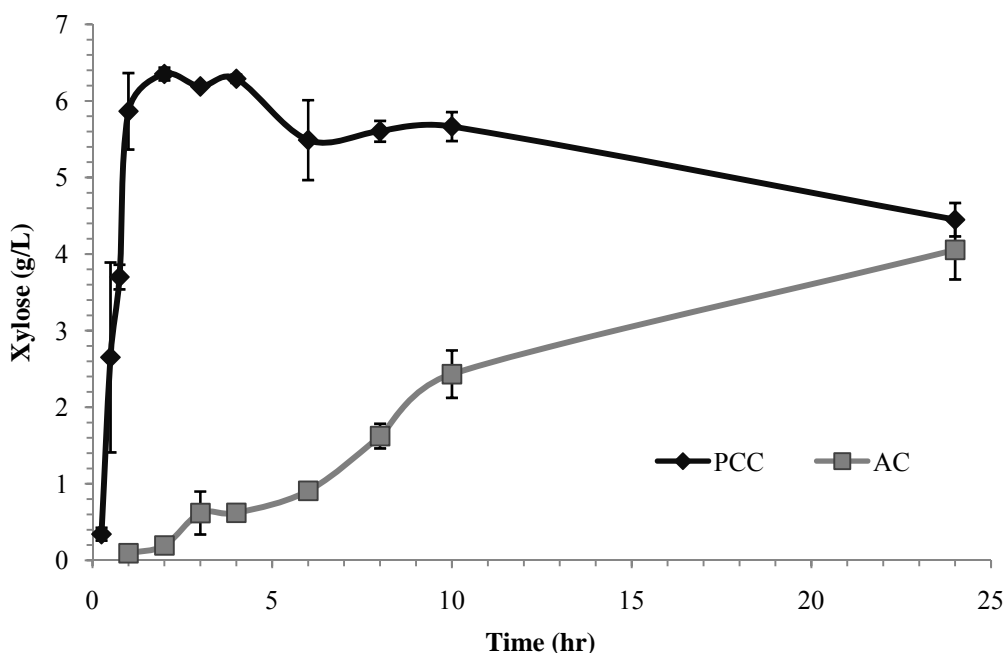


Figure 15. Comparison of PCC and AC activity with xylan at 120 °C, 650 rpm, 7.3 g/L xylan and 9% catalyst wt.

### Hemicellulose Hydrolysis with Amberlyst 15 Resin

Amberlyst 15 Resin was used as a benchmark comparison for solid acid catalyst activity and reusability. Rinsate from a room temperature rinse at one hour remained at neutral pH. A15R samples were dried at 55 °C for 5 hours before storage for later use. Birchwood xylan was hydrolyzed with A15R under the same conditions as PCC. A comparison of catalyst activity for PCC and A15R at various temperatures is shown in figure 16. Catalyst activity of A15R is similar to PCC at 120 °C but significantly lower at lower temperatures. The difference in activity at lower temperatures may be a function of xylan’s adsorption affinity to the surface of each catalyst. Similar to PCC, A15R was reduced to a fine powder following the primary hydrolysis reaction.

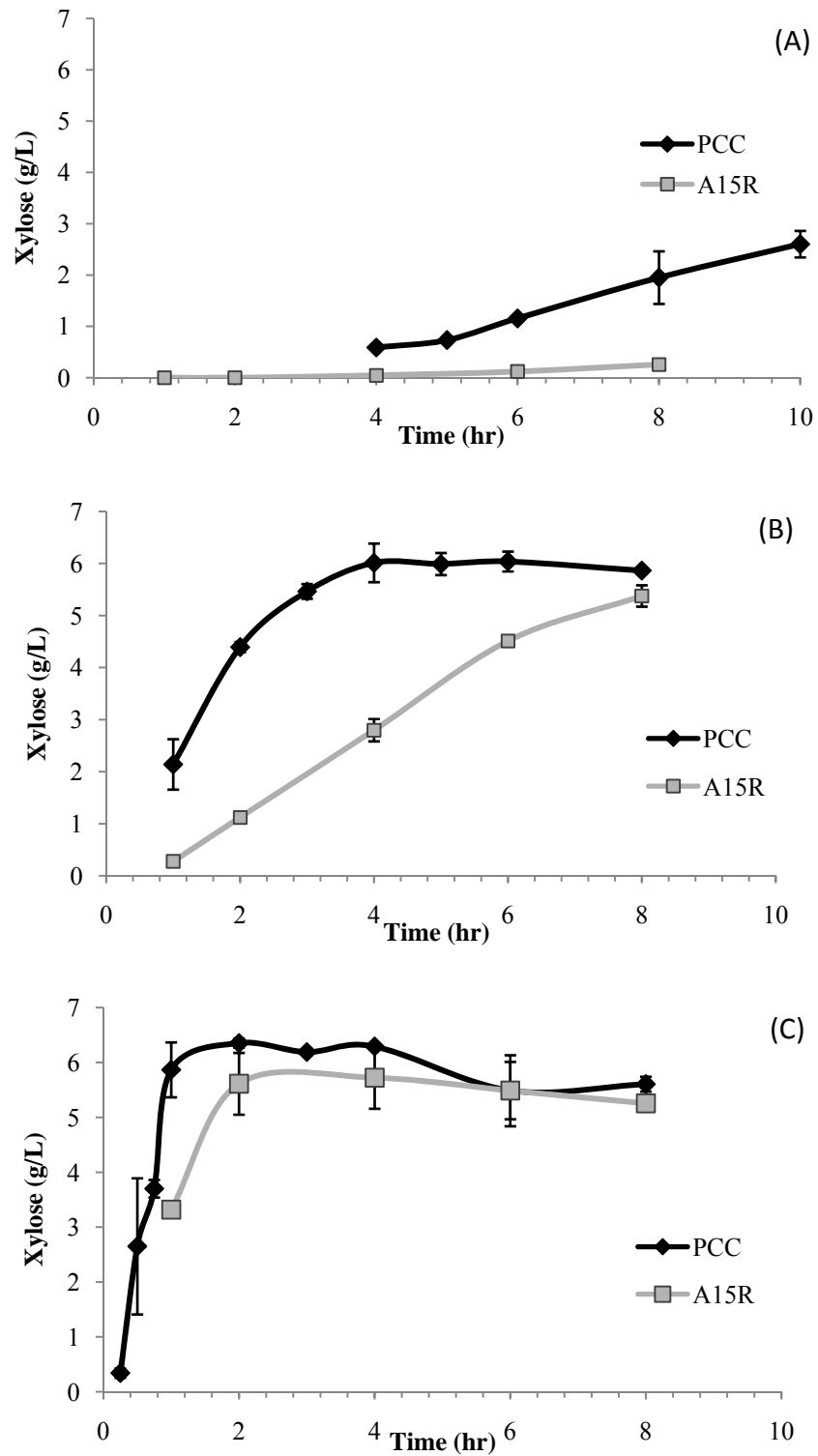


Figure 16. Comparison of PCC and A15R activity at 90 °C (A), 110 °C (B), and 120 °C (C), 7.3 g/L xylan, 650 rpm, 9% wt. catalyst.

## Reuse A15R Hemicellulose Hydrolysis

Reuse conditions for A15R were the same as PCC at 120 °C for 2 hours. Sulfonic characteristics of A15R are shown in table 3. The pore volume and radius for all A15R samples were below detection using the BET method. The difference in catalytic activity between PCC and AR15 is probably related to a difference in pore dimensions. The acid density for AR15 is greater than PCC by a factor of 10. Both catalysts show a similar reduction after the first hydrolysis reaction. Sulfur content and acid density remain relatively constant after the first hydrolysis reaction for AR15, but a steady decline occurs following each subsequent reuse for PCC. Catalyst activity over multiple hydrolysis reactions is shown in figure 17.

Table 3. A15R sulfonic characteristics (CHNS analysis) and PCC comparison

Number of Uses	Average Sulfur Content (%)	Std. Dev.	AR15 SO <sub>3</sub> H Acid Density (mmol/g)	PCC SO <sub>3</sub> H Acid Density (mmol/g)
0	15.1	0.364	4.70	0.69
1	11.8	0.046	3.68	0.43
2	11.4	0.199	3.55	0.4
3	11.0	0.070	3.42	0.33
4	10.8	0.076	3.37	0.27

After four hydrolysis reactions the activity of A15R declined by approximately 15% while PCC was rendered inactive. The differences between the two curves can possibly be attributed to differences in the quality of the catalyst support matrix. The approximate 15% decline in activity between the first and fourth A15R hydrolysis reaction is similar to the 10% drop in sulfur content shown in table 3. The carbon lattice

of the PCC is brittle and suffered severely from attrition and acid site leaching most likely due to agitation using stir bars and the close confines of the tubular reactors.

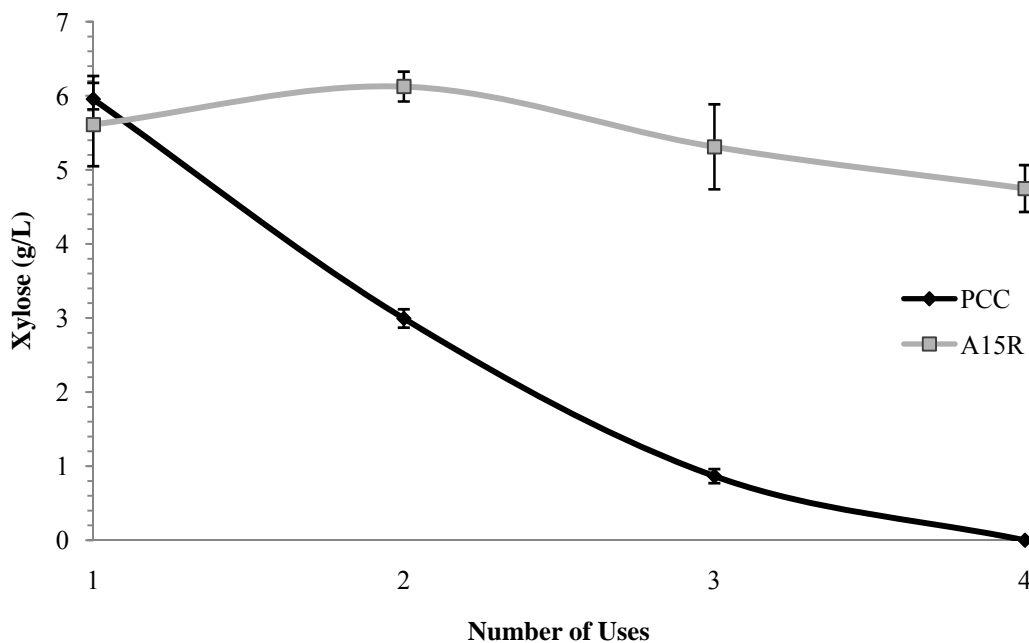


Figure 17. Comparison of PCC and A15R reuse activity with xylan at 120 °C, 2 hr, 7.3 g/L xylan, 650 rpm, 9% wt. catalyst.

The PCC sulfur content was reduced by approximately 39% between the first and fourth hydrolysis reactions as shown in table 2. Apparently, the styrene resin structure of the AR15 was more stable than the carbon lattice of the PCC. Although A15R suffered from a similar reduction in particle size, the physical characteristics remained somewhat constant over multiple reactions. The bond between SO<sub>3</sub>H and the surface of the catalyst is probably stronger for A15R than PCC.

## Reaction Rate and Agitation

Reaction agitation rates were varied in an attempt to reduce catalyst attrition due to physical wear. All prior experimentation was conducted at an agitation rate of 650 rpm. Further xylan hydrolysis trials with PCC at the maximum yield temperature of 120 °C were conducted at 500 and 250 rpm. Individual reactors were removed at time intervals between 0.25 and 2 hours and product concentration were measured via HPLC analysis. The slope of the linear increase in xylose production over time was used to determine the reaction rate. The effect of agitation speed on rate of reaction is shown in figure 18.

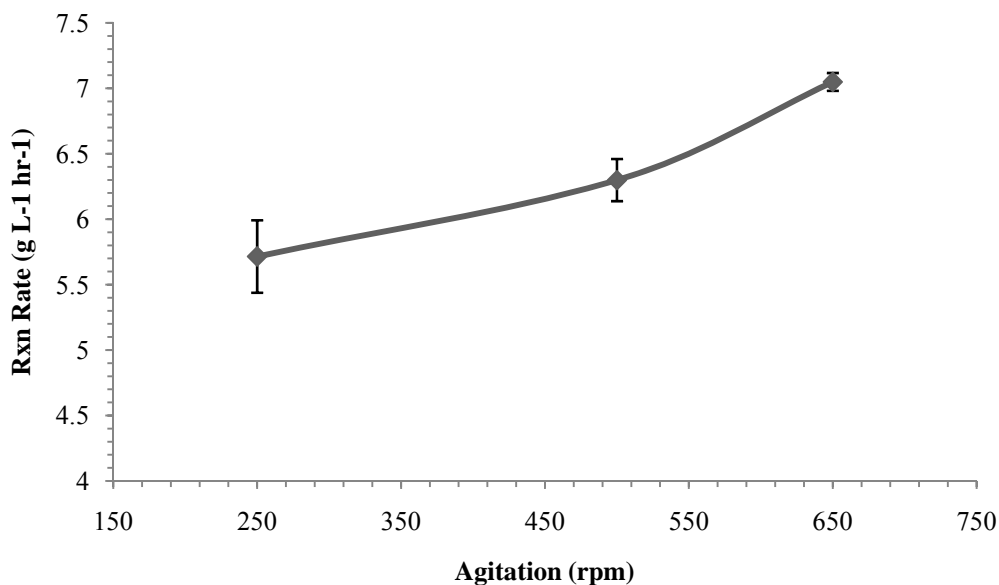


Figure 18. Effect of agitation rate on reaction rate of PCC xylan hydrolysis at 120 °C, 7.3 g/L xylan, 9% wt. catalyst.

The positive relationship between agitation rate and rate of xylan hydrolysis suggests that the reaction is mass transfer limited. Hydrolysis reactions at higher agitation rates resulted in a greater reduction in catalyst particle size, which could contribute to the rate of deactivation following multiple uses. The flat surface of the solution would begin to break and rise along the walls of the tubular reactor at agitation rates larger than 650 rpm. In order to maintain uniform reaction conditions between all trials, reaction rates were not measured for agitation speeds greater than 650 rpm.

### **Hemicellulose Reaction Kinetics**

The first order rate law was rewritten to describe the rate constant  $k$  as the slope of the linear curve of  $\ln(A/A_0)$  as a function of time. The average rate constant at each of the experimental temperatures (90 °C, 110 °C, and 120 °C) is shown in figure 19. The constant  $A_0$  represents the initial xylan concentration of 7.3 g/L and  $A$  represents the xylan concentration at any given time  $t$ . The activation energy was calculated from the Arrhenius equation using average  $k$  values and the slope shown in figure 20.

The activation energy for the formation of xylose as a product of PCC xylan hydrolysis was calculated to be approximately 141 kJ/mol. This value falls within the range of reported activation energy range of 130-170 kJ/mol for the hydrolysis of hardwood hemicellulose with sulfuric acid (Lu and Mosier 2008; Yat et al. 2007). The frequency factor determined by the intercept of the linear function in figure 20 was calculated to be approximately  $2.3 \times 10^{15} \text{ s}^{-1}$ .

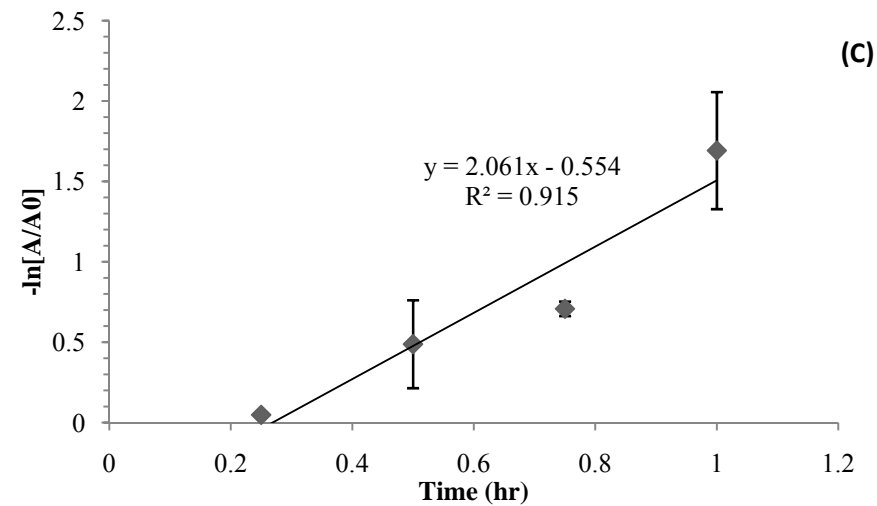
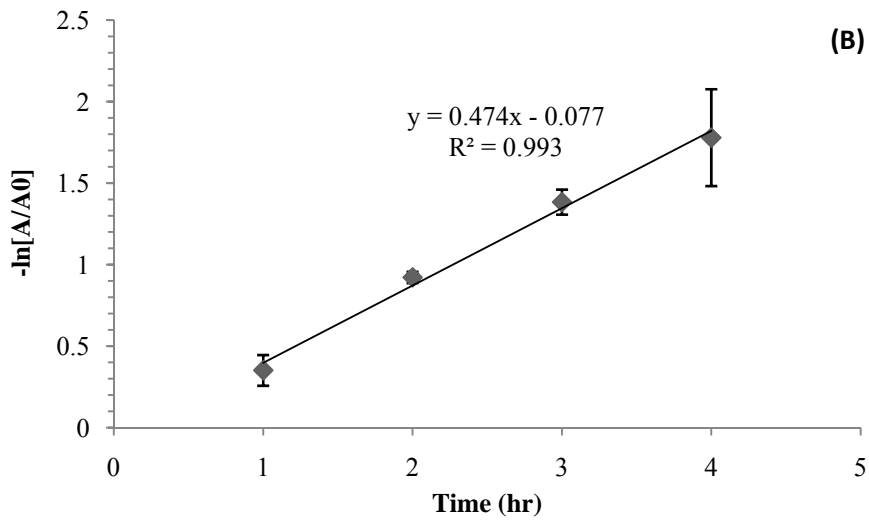
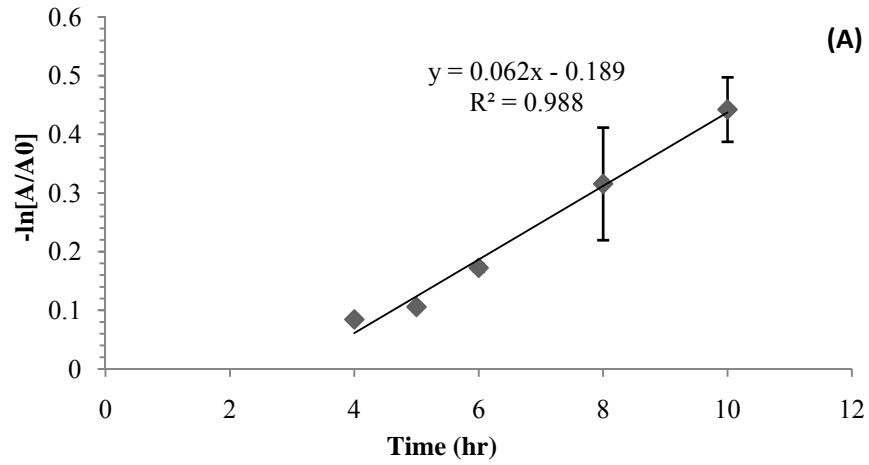


Figure 19. Average rate constant  $k$  (slope) as a function of change in concentration and time for 90 °C (A), 110 °C (B), and 120 °C (C) for an initial xylan concentration of 7.3 g/L, PCC catalyst.

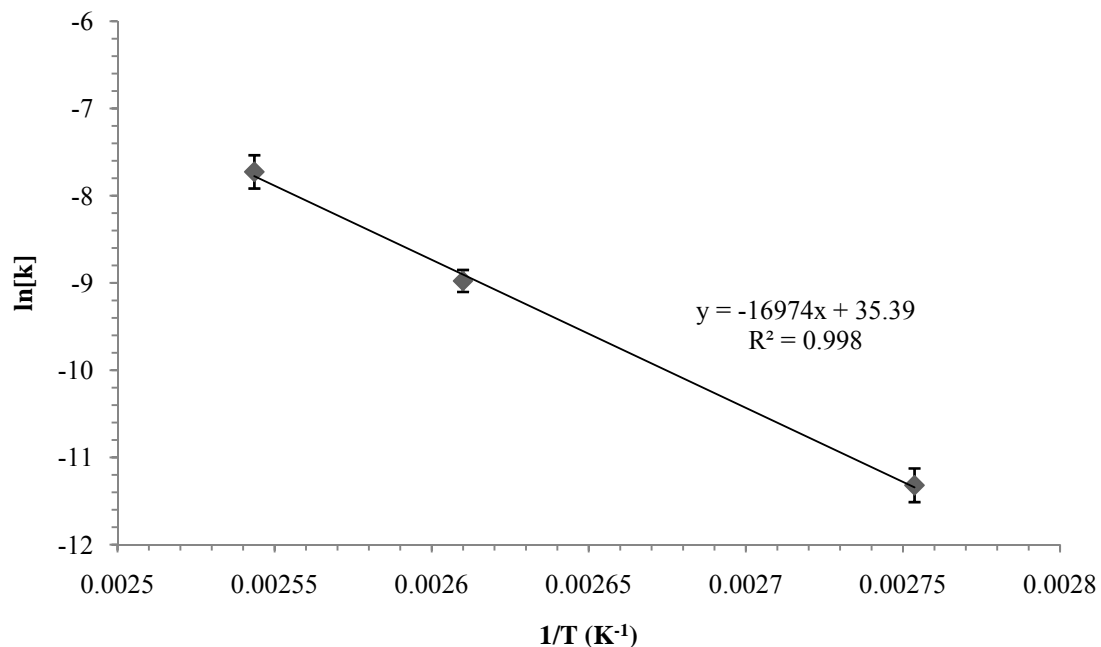


Figure 20. Activation energy  $E_a$  of xylose formation as a function of  $T^{-1}$  and  $\ln(k)$  for initial xylan concentration of 7.3 g/L, PCC catalyst.

The activation energy for the hydrolysis of xylan to xylose with A15R was also calculated from  $k$  values with the Arrhenius equation. The average rate constant for A15R at 90, 110, and 120 °C is shown in figure 21 while the activation energy is shown as a function of the slope in figure 22. The activation energy and frequency factor for A15R were calculated to be 121 kJ/mol and  $3.1 \times 10^{24} \text{ s}^{-1}$  respectively by rearranging the Arrhenius equation to fit the linear relationship shown in figure 22. The reaction rate in terms of weight of xylan reacted per weight of catalyst per hour for both PCC and A15R was calculated by the following rate law:

$$-r_A = kC_A = CA_0VW^{-1} dX/dt$$

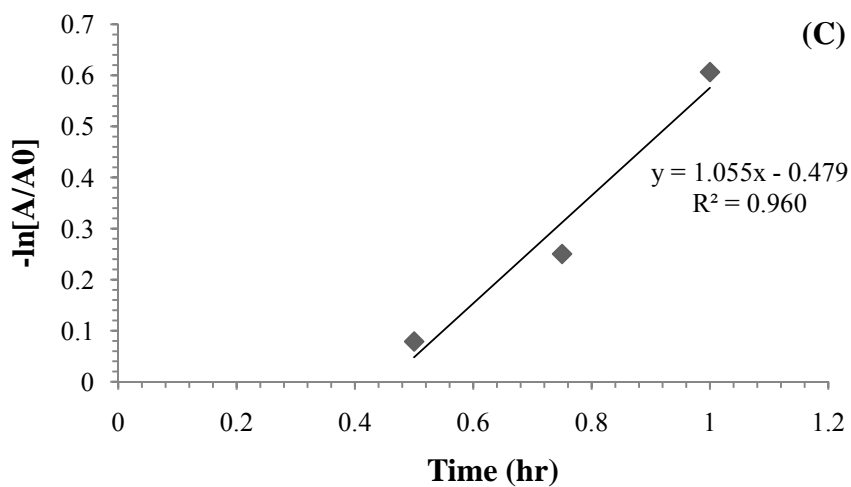
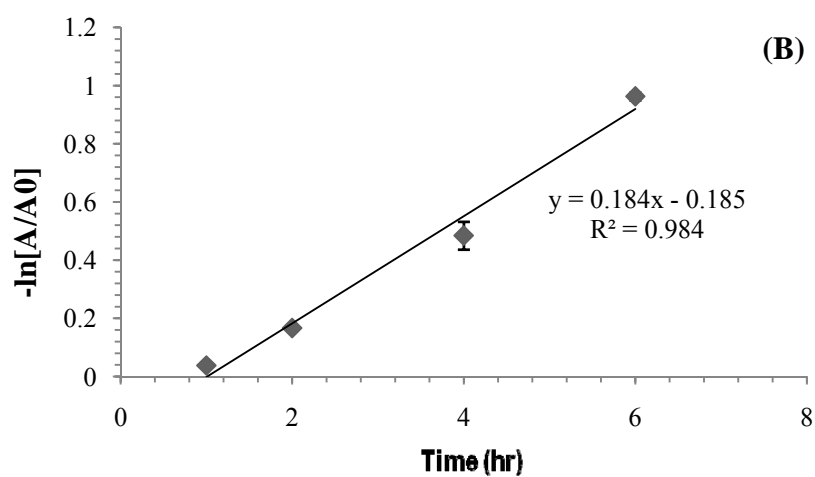
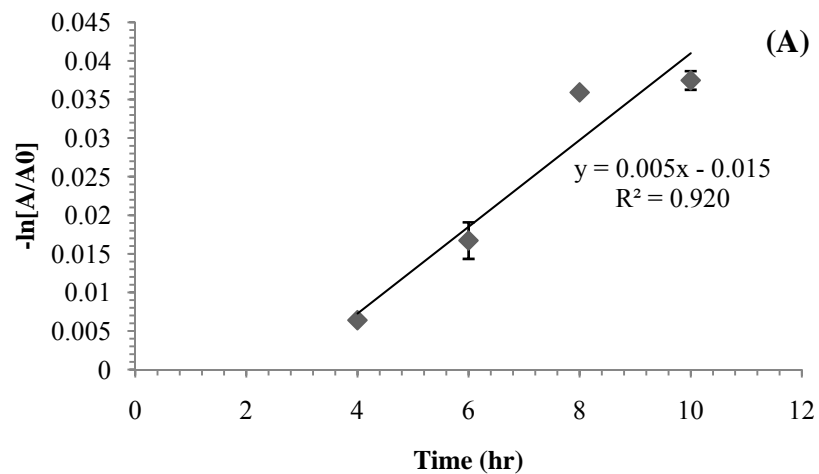


Figure 21. Average rate constant  $k$  (slope) as a function of change in concentration and time for 90 °C (A), 110 °C (B), and 120 °C (C) for an initial xylan concentration of 7.3 g/L, A15R catalyst.

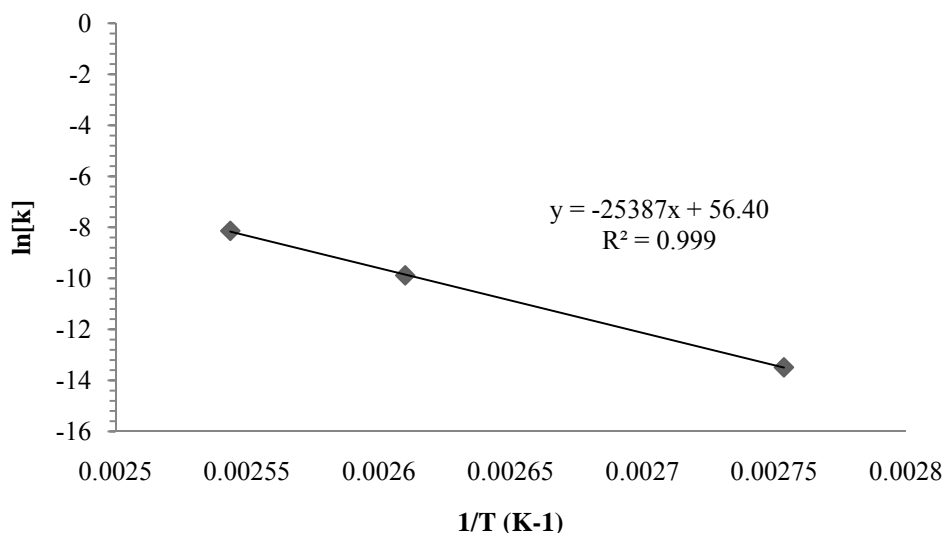


Figure 22. Activation energy  $E_a$  of xylose formation as a function of  $T^{-1}$  and  $\ln(k)$  for initial xylan concentration of 7.3 g/L, PCC catalyst.

In the rate law equation,  $CA_0$  represents the initial xylan concentration.  $V$  represents the volume of the xylan solution and  $W$  represents the weight of the solid acid catalyst.  $X$  represents fractional convergence of xylan to xylose and  $t$  represents time. The reaction rates for PCC and A15R hydrolysis with an initial xylan concentration of 7.3 g/L are shown in table 4. The lower reaction rates of A15R are probably due to a lower adsorption affinity for xylan.

Table 4. Reaction rate of xylan hydrolysis with PCC and A15R catalysts

Temperature (°C)	PCC Reaction Rate ( $g_{\text{xylan}} g_{\text{PCC}}^{-1} \text{hr}^{-1}$ )	A15R Reaction Rate ( $g_{\text{xylan}} g_{\text{A15R}}^{-1} \text{hr}^{-1}$ )
90	3.5	0.4
110	18.6	8.5
120	70.4	55.3

Initial hemicellulose concentrations were varied to determine if the reaction rate was affected by the xylan concentration and adsorptivity of the PCC catalyst. The effect of initial concentration on reaction rate for PCC at 120 °C is shown in figure 23. The greatest reaction rate was achieved at initial xylan concentrations of 7.3 g/L. The reaction rate plateaued at 7.3 g/L of xylan and subsequently declined as the initial xylan concentration increased. This suggests that the reaction rate is limited by the adsorptivity of the catalyst or oligomer fragments inhibited the catalytic reaction. Oligomers generated as intermediary transition products or by the reformation of monomers could potentially block active acidic sites on the catalyst surface.

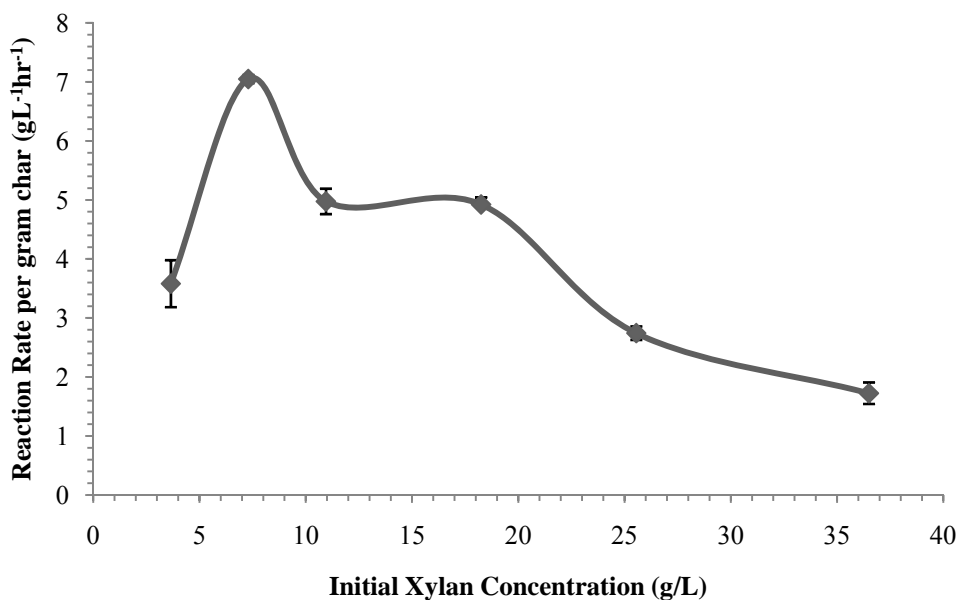


Figure 23. Reaction rate per gram of PCC as a function of initial xylan concentration at 120 °C, 650 rpm, 9% wt. catalyst.

## CHAPTER 6

### LEVOGLUCOSAN RESULTS AND DISCUSSION

#### PCC Hydrolysis of Model Levoglucosan

HPLC chromatograms were used to determine the concentration of levoglucosan and glucose following levoglucosan hydrolysis. A model compound of levoglucosan was used for the preliminary hydrolysis reaction with PCC. The glucose and levoglucosan peaks were identified given the retention time of a 10 g/L glucose and 1 g/L levoglucosan standard. A thermal control was used to verify that hydrolysis did not occur without the catalyst. Figure 24 shows the matching retention times (approximately 10.8 minutes for glucose and 14.5 minutes for levoglucosan) between the glucose standard (A), levoglucosan standard (B), products following 17 hr. hydrolysis of levoglucosan at 120 °C (C), and as well as the absence of glucose in the thermal control of 17 hrs at 120 °C (D). The model compound of levoglucosan was found to almost completely convert to glucose, while the thermal control showed no change in levoglucosan concentration.

The catalyst activity of sulfonated PCC with levoglucosan is further illustrated in figure 25, which shows the change in concentration for each compound with respect to time at 120 °C. Approximately 80% conversion of levoglucosan to glucose was achieved after 2 hours.

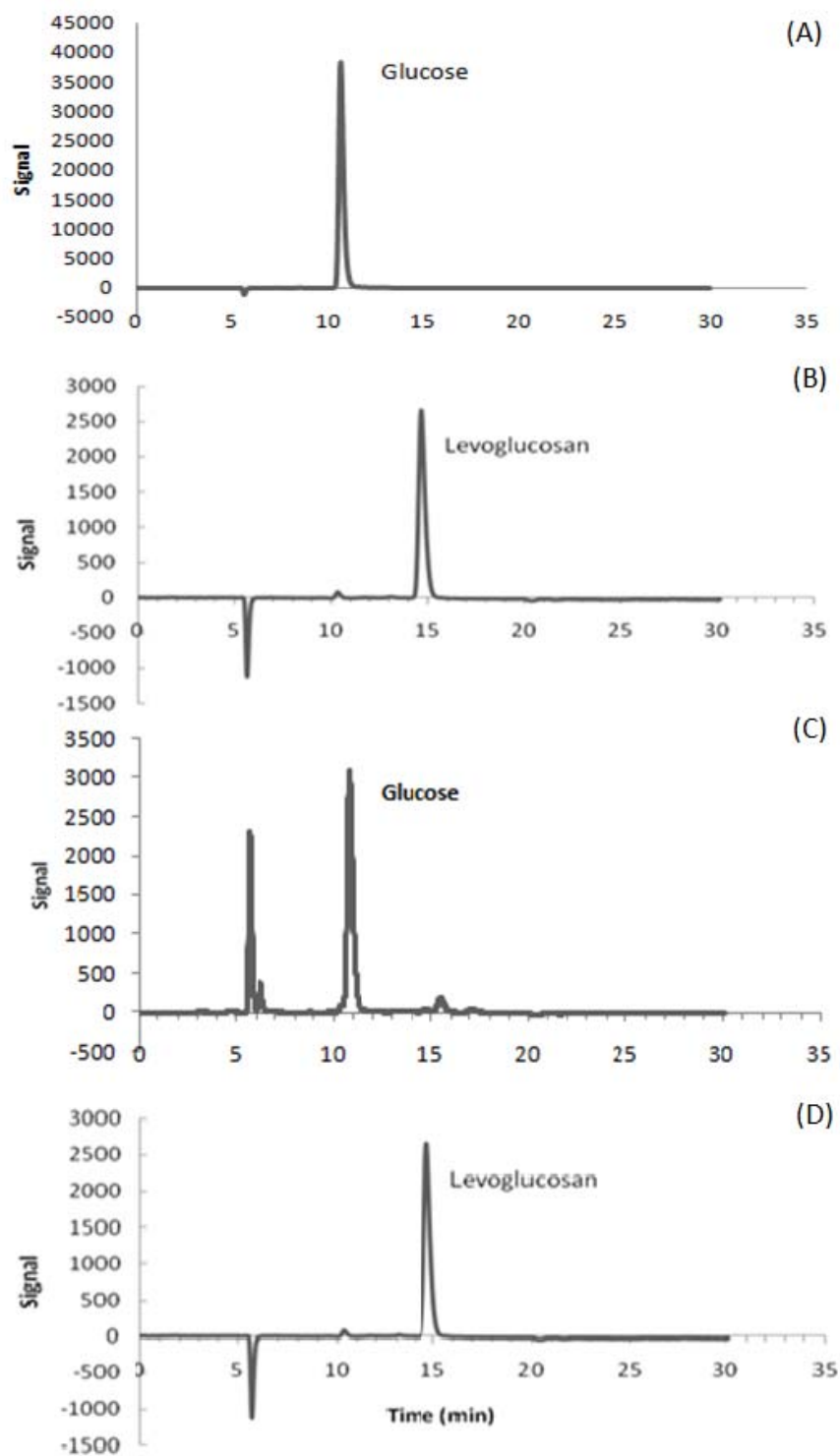


Figure 24. HPLC chromatograms of 10 g/L glucose standard (A), 1 g/L levoglucosan standard (B), 17 hr, 123 °C levoglucosan hydrolysis products (C), and 17 hr, 123 °C levoglucosan thermal control (D).

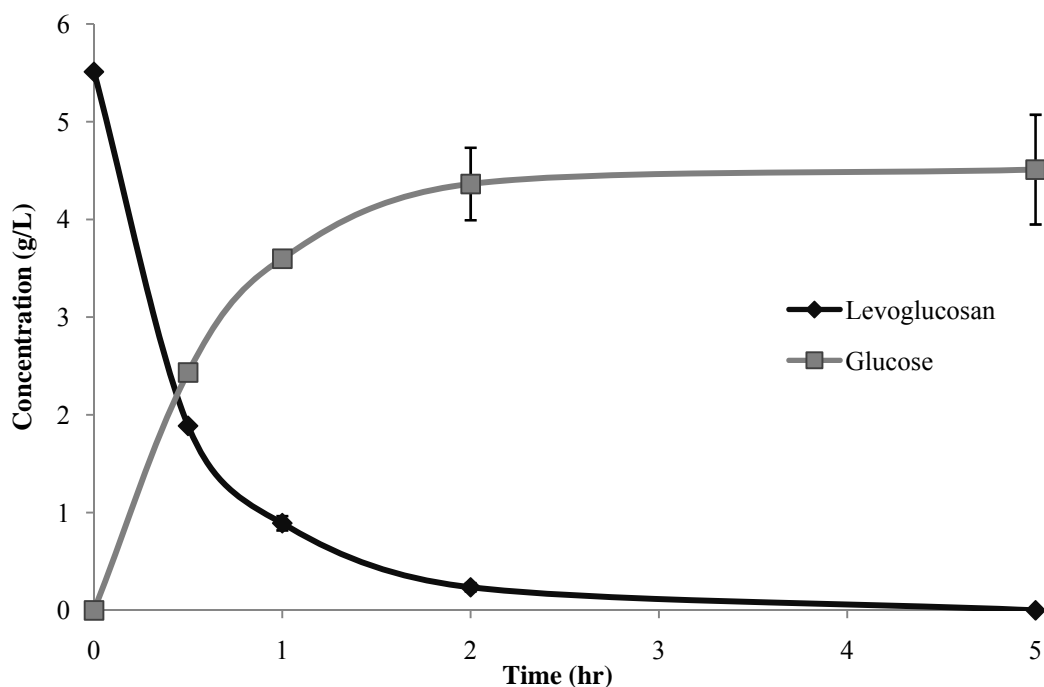


Figure 25. Model compound levoglucosan with sulfonated PCC hydrolysis results, 120 °C, 5.5g/L levoglucosan, 650 rpm, 9% wt. catalyst.

### Bio-oil Characterization

Bio-oil samples were collected from both fast pyrolysis (FP) and in-line-condensation fast pyrolysis (ILC) methods. De-ionized water was added to the FP samples to bring the water concentration from approximately 20% wt. to 50% wt. Samples were then centrifuged at 3500g for 15 minutes at room temperature and the aqueous phase was extracted for HPLC analysis. The aqueous phase of the ILC bio-oil samples was drawn directly from the pyrolysis reactor for HPLC analysis. Initial sugar concentrations for the aqueous phase ILC and FP samples as well as the non aqueous FP oil are shown in table 5.

Table 5. Initial sugar concentrations for aqueous and non aqueous phase FP oil

Oil	Levoglucosan (g/L)	Xylose (g/L)	Glucose (g/L)	Acetate (g/L)	5-HMF (g/L)	Furfural (g/L)	Water (%)
ILC (aq)	169.9	3.8	0.0	79.8	1.9	1.3	50
FP (aq)	165.6	5.9	1.1	80.4	1.7	1.1	50
FP	266.8	10.6	2.0	125.8	3.0	2.0	20

The average levoglucosan concentration for the FP and ILC methods was approximately the same at 165.48 g/L and 170 g/L respectively. The ILC method is therefore the more efficient method for producing aqueous phase bio-oil as it removes the separation and extraction step required to obtain the aqueous phase of the FP oil.

### **Bio-oil Hydrolysis with PCC**

An aqueous phase ILC sample with approximately 153 g/L of levoglucosan was hydrolyzed with sulfonated PCC char. The sample had an approximate water/oil ratio of 50%, and had not been filtered. Ten mL of the aqueous phase bio-oil was combined with 1 g of catalyst and heated to 120 °C over time intervals ranging from 1 to 24 hours. The resulting sugar concentrations are shown in table 6. There appears to be a sharp decline in levoglucosan within the first hour of hydrolysis, but the concentration of glucose does not seem proportional to values found in the model compound trials. Furthermore, the final concentrations for all sugars after 24 hours are almost identical to the thermal control. The samples themselves developed a solid disc of particulate matter that settled on top of the solution, as well as a thick, hard film on the stir bars which can be seen in

figure 26. This suggests polymerization may be occurring during the hydrolysis reaction, possibly forming solid humans, which reduces the total glucose yield.

Table 6. ILC-Bio-oil hydrolysis product yield concentrations at various time intervals at 120 °C.

Time (hr)	Levoglucosan (g/L)	Glucose (g/L)	Xylose (g/L)	Arabinose (g/L)	Acetate (g/L)	5-HMF (g/L)
0	169.9	0.0	3.8	0	79.8	1.9
1	45.94	10.87	8.6	0	70.02	1.17
2	16.62	15.03	9.99	2.94	58.57	0.45
3	13.53	16.28	11.34	3.65	60.57	0.66
4	10.02	16.36	11.84	3.95	60.09	0.31
6	6.63	15.6	11.76	3.97	56.39	0
8	6.08	15.82	11.99	3.99	57.01	0
24	2.89	14.16	9.96	3.13	53.19	0
24 hr Control	3.98	14.61	10.57	3.36	56.11	0

In order to prevent polymerization, further trials included ethanol dilution of FP bio-oil in an attempt to simultaneously hydrolyze levoglucosan and esterify organic acids and aldehydes in the bio-oil. FP bio-oil samples were taken directly from the pyrolysis reactor and prepared for PCC hydrolysis in ethanol. Two controls were included: a thermal control consisting of only bio-oil and ethanol, and a second control consisting of only bio-oil and PCC catalyst.



Figure 26. Solid disc formed over the hydrolysis products of ILC aqueous phase bio-oil and PCC catalyst.

The second control group created a thick tar-like paste that could not be filtered nor analyzed. Table 7 shows the average concentrations of various compounds found in fast pyrolysis oil before and after solid acid catalyst hydrolysis. The first control group and both experimental groups showed little difference in final sugar concentrations. Although there was a 30 - 40% decrease in levoglucosan concentration, there was not a corresponding increase in glucose or further decomposition compounds such as 5-HMF.

Table 7. Average concentration of fast-pyrolysis oil compounds before and after hydrolysis with solid acid catalysts.

Sample Group	Time (hr)	Levoglucosan (g/L)	Xylose (g/L)	Glucose (g/L)	Acetate (g/L)	5-HMF (g/L)	Furfural (g/L)
Bio-Oil	0	247.66	9.17	1.6	118.92	2.84	1.02
Bio-Oil Etoh	0	200.65	0.27	0	95.49	2.99	0.98
Bio-Oil Etoh	5	147.24	7.94	2.47	107.72	2.61	1.82
AC Bio-Oil Etoh	5	152.22	7.87	2.74	103.71	2.57	1.38
PCC Bio-Oil Etoh	5	165.05	7.66	4.61	102.79	2.82	0

HPLC analysis also showed a number of unidentified peaks for all bio-oil hydrolysis samples. These peaks may represent the formation of esters or intermediate oligosugars leading to the formation of levulinic acid. An example of these unknown peaks from an HPLC analysis of PCC bio-oil and ethanol hydrolysis reaction after 5 hours at 120 °C is shown in figure 27. These peaks did not appear at any of the known retention times for any standard curves available for compound identification and quantification through HPLC analysis. These peaks appeared at similar but not identical retention times for samples with and without PCC. Gas chromatography and mass spectrometry analysis (GC/MS) was used in an attempt to identify these unknown compounds.

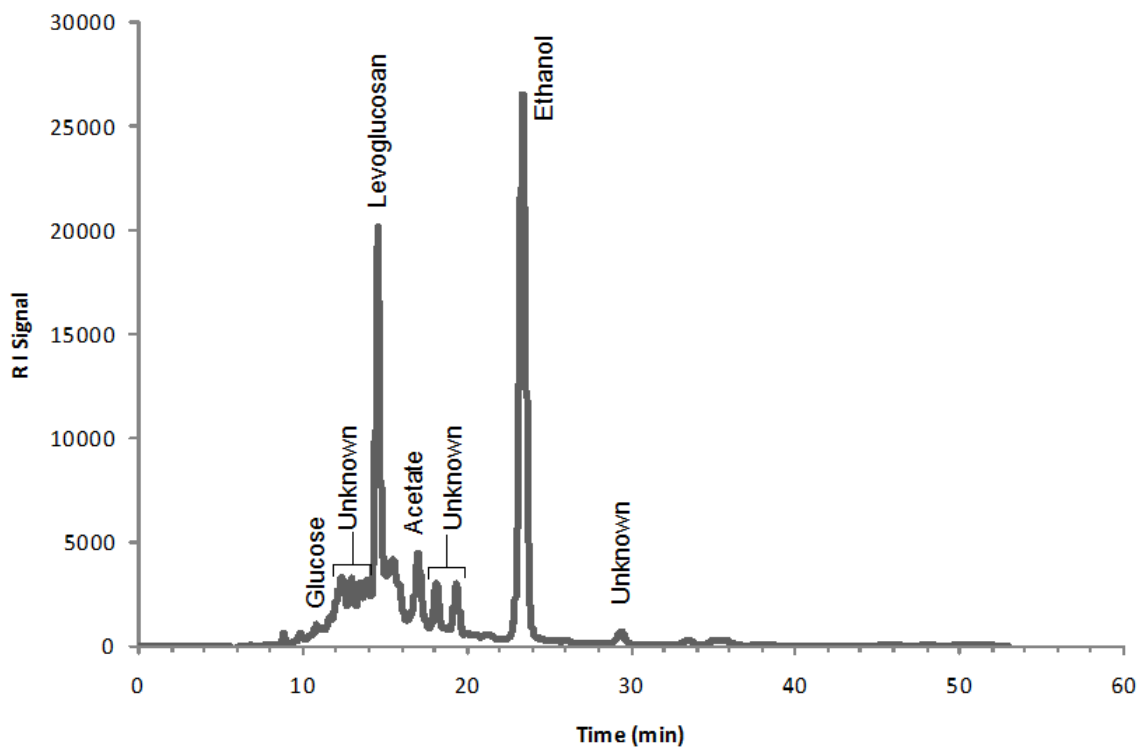


Figure 27. HPLC analysis of PCC bio-oil ethanol hydrolysis, 5 hrs, 120 °C, 650 rpm, 2.5% wt. catalyst

The GC/MS chromatograph for bio-oil samples and controls before and after PCC hydrolysis is shown in figure 28. All samples are fast pyrolysis bio-oil diluted to 50% in ethanol. Many of the peaks that appear in the bio-oil sample that was reacted with the PCC catalyst also appear in the bio-oil control. Peak 1 in figure 28 has a retention time of 1.85 minutes with a 90% certain identity of ethyl acetate, the presence of which confirms a successful esterification reaction. Peak 2 with a retention time of 8.24 minutes has been identified as ethyl orthoformate with 78% certainty. Peak 3 has a retention time of 9.90 minutes and GC/MS analysis has determined a 59% certainty that this peak represents 1,1-diethoxy-pentane.

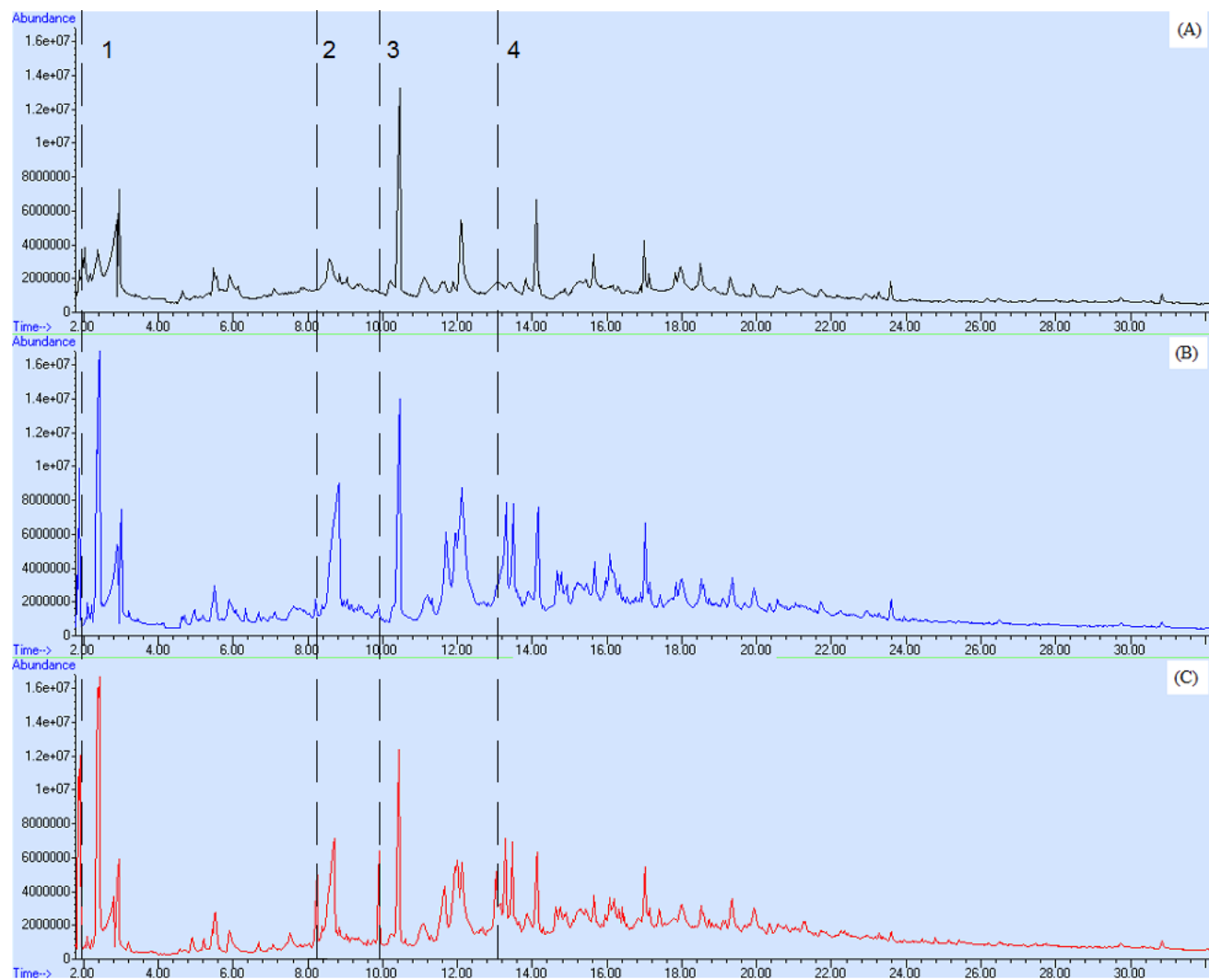


Figure 28. GC/MS analysis of FP bio-oil before hydrolysis 25 °C (A), FP bio-oil control 5 hr. (B), FP bio-oil and PCC 5hr. 120 °C (C)

Although peaks 2 and 3 are present in the bio-oil sample reacted with heat alone (B), the peak area is significantly larger in the reaction with PCC. Although GC/MS analysis could not quantify the specific concentration of the compounds associated with peaks 2 and 3, the difference in abundance suggests that PCC generated a larger concentration of these compounds. Peak 4 has a retention time of 13.15 minutes with a 32% certain identity of 1,1,1-triethoxy-ethane, which was not present in the sample reacted without PCC (B). Although the identity of these peaks is not 100% certain, all compounds appear to be ethers or esters.

## CHAPTER 7

### CONCLUSIONS AND FUTURE RESEARCH

#### Hemicellulose

Sulfonic acid functional groups were formed on the surface of pine chip biochar, and the solid acid catalyst successfully hydrolyzed model compounds representing hemicellulose to fermentable sugars. The reaction conditions, 2 hours and 120 °C, were similar to hemicellulose hydrolysis reactions with a dilute liquid acid with an 88% yield as compared to liquid catalysts under the same conditions. Product yields were 40-50% higher than enzymatic hydrolysis reactions of the same time interval, although the solid acid catalyst reactions required higher temperatures of 120 °C as opposed to 60 °C. Furthermore, the PCC showed evidence of high xylose yields without the production of 5-HMF. The sulfonated pine chip biochar solid acid catalyst had a greater activity than commercially available Amberlyst 15 especially at temperature below 120 °C. However, the activity of the Amberlyst 15 remained relatively consistent over multiple uses while the sulfonated biochar activity steadily declined. Although the sulfonated biochar was safer to handle than liquid acid catalysts, sulfonation techniques required large quantities of water resulting in an acidic waste stream.

Acidic rinsate streams could be avoided by changing the sulfonation method from liquid sulfuric acid to gaseous sulfur trioxide. Excess sulfonic groups could be swept from the char via a nitrogen gas stream, which could then be purified by a wet scrubber. The decline in biochar catalyst activity may have been a result of physical attrition of the

char. High agitation rates, the small volume of the bench scale reactors, and large contact area between the stir bars, catalyst, and tube walls all contributed to the rapid physical deformation of the catalysts. Increasing the temperature of the char generation pyrolysis reaction could result in a stronger carbon lattice.

Physical stability of the char could be maintained by reducing agitation rates at the cost of a similar reduction in maximum product yield. A continuous flow reactor could reduce the rate of physical attrition, but would not prevent leaching of  $\text{SO}_3\text{H}$  from the surface of the catalyst. Sulfonic leaching may also be attributed to the physical instability of the biochar. A stronger carbon lattice generated through higher pyrolysis temperatures combined with gaseous sulfur trioxide sulfonation may reduce sulfonic leaching.

Physical instability, extensive rinsing associated with sulfonation, and rapid activity decline over multiple uses have diminished the commercial potential of this solid acid catalyst generated by through the methods of this study.

### **Levogluconan and Bio-oil**

Sulfonated pine chip biochar was equally capable at hydrolyzing model compound levogluconan to fermentable glucose. Hydrolysis of levogluconan in fast pyrolysis bio-oil in a water-rich medium was less successful due to the apparent polymerization of glucose and oligosugars to solid humins. Although some glucose was recovered, the quantity was not proportional to what was predicted using the model compound. Simultaneous esterification and hydrolysis reactions effectively removed any evidence of polymerization, but glucose yields were still low even at temperatures below  $130\text{ }^\circ\text{C}$  where glucose should be the primary product. There was evidence of additional ester formation in the presence of the sulfonated PCC catalyst. Although glucose was not

generated in expected quantities, the formation of ethers and esters suggests other potential applications of the sulfonated PCC catalyst. Proper identification of these ethers and esters would require the purchase of additional standards to determine retention times and standardized curves for GSMS analysis.

The in-line-condensation method (ILC) of fast pyrolysis was proven to be a more efficient method of levoglucosan production and extraction to the aqueous phase. By spraying water directly to the fast pyrolysis condenser, a levoglucosan rich aqueous phase bio-oil stream was available directly from the reactor. Average levoglucosan concentrations from this ILC aqueous phase were slightly greater than concentrations extracted from fast pyrolysis bio-oil via water addition and centrifuge phase separation.

The sulfonated pine chip solid acid catalyst is not ready for commercial application in this phase of research. However, evidence was shown of the catalyst's applicability across both thermochemical and biochemical biomass conversion platforms in the generation of both esters and fermentable sugars. Commercial applications may be possible if further research can resolve the problems of physical instability and deactivation over multiple uses.

## REFERENCES

- Amidon, T. E. and S. Liu (2009). "Water-based woody biorefinery." *Biotechnology Advances* 27(Compendex): 542-550.
- Bennett, N. M., Helle, S. S., and Duff, J. B. (2009). "Extraction and hydrolysis of levoglucosan from pyrolysis oil." *Bioresource Technology* 100(23), 6059-6063
- Boateng, A. A., Dugaard, D. E. et al. (2007). "Bench-scale fluidized-bed pyrolysis of switchgrass for bio-oil production." *Industrial and Engineering Chemistry Research* 46(Compendex): 1891-1897.
- Carapito, R., Carapito, C., Jeltsch, J. M., and Phalip, V. (2009) "Efficient hydrolysis of hemicellulose by a *Fusarium graminearum* xylanase blend produced at high levels in *Escherichia coli*." *Bioresource Technology* 100(2), 845-850
- Cherubini, F. (2010). "The biorefinery concept: Using biomass instead of oil for producing energy and chemicals." *Energy Conversion and Management* 51(Compendex): 1412-1421.
- Dehkhoda, A. M., West, A. H., et al. (2010). "Biochar based solid acid catalyst for biodiesel production." *Applied Catalysis A: General*, 382(Compendex): 197-204.
- Fatih Demirbas, M. (2009). "Biorefineries for biofuel upgrading: A critical review." *Applied Energy* 86(Compendex): S151-S161.
- Gunawan, R. Li, X., et al. (in press 2011) "Hydrolysis and glycosidation of sugars during the esterification of fast pyrolysis bio-oil." *Fuel*.
- Helle, S., Bennett, N. M., Lau, K., Matsui, J. H., and Duff, S. J. B. (2007). "A kinetic model for production of glucose by hydrolysis of levoglucosan and cellobiosan from pyrolysis oil." *Carbohydrate Research*, 342, 2365-2370.
- Hu, X. and Li, C. Z., (2011). "Levulinic esters from the acid-catalysed reactions of sugars and alcohols as part of a bio-refinery." *Green Chemistry*, 13, 1676-1679.
- Huber, G. W., Iborra, S., and Corma, A. (2006). "Synthesis of transportation fuels from biomass: Chemistry, catalysts, and engineering." *Chemical Reviews*, 106(9), 4044-4098.
- Jin, Q., Zhang, H., Yan, L., Qu, L. and Huang, H. (2011) "Kinetic characterization for hemicellulose hydrolysis of corn stover in dilute acid cycle spray flow-through reactor at moderate conditions." *Biomass and Bioenergy*, (Compendex), 1-7.

- Kulkarni, M. G., Gopinath, R., Meher, L. C., and Dalai, A. K. (2006). "Solid acid catalyzed biodiesel production by simultaneous esterification and transesterification." *Green Chemistry*, 8, 1056 - 1062.
- Kumar, P., Barrett, D. M., Delwiche, M. J., and Stroeve, P. (2009a). "Methods for pretreatment of lignocellulosic biomass for efficient hydrolysis and biofuel production." *Industrial and Engineering Chemistry Research*, 48(8), 3713-3729.
- Kusema, B. T., Hilmann, G., Mäki-Arvela, P., Willför, S., Holmbom, B., Salmi, T., and Murzin, D. Y. (2010). "Selective hydrolysis of arabinogalactan into arabinose and galactose over heterogeneous catalysts." *Catalysis Letters*, 141(3), 408-412.
- Lavarack, B. P., Griffin, G. J., and Rodman, D. (2000). "Measured kinetics of the acid-catalyzed hydrolysis of sugar cane bagasse to produce xylose." *Catalysis Today*, 63(2-4), 257-265.
- Lopez, D. E., Goodwin Jr, J. G., and Bruce, D. A. (2007). "Transesterification of triacetin with methanol on Nafion<sup>®</sup> acid resins." *Journal of Catalysis*, 245(2), 381-391.
- Lu, Y., and Mosier, N. S. (2008). "Kinetic modeling analysis of maleic acid-catalyzed hemicellulose hydrolysis in corn stover." *Biotechnology and Bioengineering*, 101(6), 1170-1181.
- Maggi, R., Sartori, G., Oro, C., and Soldi, L. (2008). "Fine chemical synthesis through supported bases." *Current Organic Chemistry*, 12(7), 544-563.
- Merino, S. T., and Cherry, J. (2007). "Progress and Challenges in Enzyme Development for Biomass Utilization." *Advanced Biochemical Engineering/Biotechnology*, 108, 95-120.
- Mosier, N., Wyman, C., Dale, B., Elander, R., Lee, Y.Y., Holtzapple, M., and Ladisch, M. (2005). "Features of promising technologies for pretreatment of lignocellulosic biomass." *Bioresource Technology*, 96(6), 673-686
- Okuhara, T. (2002). "Water-tolerant solid acid catalysts." *Chemical Reviews*, 102(10), 3641-3666.
- Pasias, S., Barakos, N., Alexopoulos, C., and Papayannakos, N. (2006). "Heterogeneously catalyzed esterification of FFAs in vegetable oils." *Chemical Engineering and Technology*, 29(11), 1365-1371.
- Shibasaki-Kitakawa, N., Honda, H., Kuribayashi, H., Toda, T., Fukumura, T., and Yonemoto, T. (2007). "Biodiesel production using anionic ion-exchange resin as heterogeneous catalyst." *Bioresource Technology*, 98(2), 416-421.

- Shu, Q., J. Gao, et al. (2010). "Synthesis of biodiesel from waste vegetable oil with large amounts of free fatty acids using a carbon-based solid acid catalyst." *Applied Energy* 87(Compendex): 2589-2596.
- Sluiter, A., Hames, B., Ruiz, R., Scarlata, C., Sluiter, J., and Templeton, D. "Determination of sugars, byproducts, and degradation products in liquid fraction process samples." Technical Report. NREL/TP-510-42623. January 2008.
- Teleman, A., Larsson, P. T., and Iversen, T. (2001) "On the accessibility and structure of xylan in birch kraft pulp." *Cellulose*, 8, 209-215
- Tessini, C., Vega, M., Müller, N., Bustamante, L., Baer, D. V., Berg, A., and Mardones, C. (2011). "High performance thin layer chromatography determination of cellobiosan and levoglucosan in bio-oil obtained by fast pyrolysis of sawdust." *Journal of Chromatography A*, 1218, 3811-3815.
- Xu, Q., Yang, Z., Yin, D., and Zhang, F. (2008) "Synthesis of chalcones catalyzed by a novel solid sulfonic acid from bamboo." *Catalysis Communications*, 9(7), 1579-1582.
- Yat, S. C., Berger, A., and Shonnard, D. R. (2007) "Kinetic characterization for dilute sulfuric acid hydrolysis of timber varieties and switchgrass." *Bioresource Technology*, 99, 3855-3863.
- Yu, Z., and Zhang, H. (2003). "Ethanol fermentation of acid hydrolyzed cellulosic pyrolysate with *Saccharomyces cerevisia*." *Bioresource Technology*, 90(1), 95-100.

## **APPENDIX A**

### **HPLC STANDARD CURVE GENERATION**

A standard curve for levoglucosan in the range of 5 – 25 g/L was prepared from solid model compound levoglucosan. A known weight of levoglucosan was dissolved into a known volume of de-ionized water and sampled for HPLC analysis to determine column retention time and peak area for a given concentration. The standard curve was generated by plotting the concentration of levoglucosan against the corresponding peak area as shown in figure A.1. The standard curve was verified by analyzing another known concentration of levoglucosan within the standard curve range. All other compounds, such as xylose, glucose, acetate, ethanol, 5-HMF, and furfural had existing curves available on the HPLC prepared by Sarah Lee, Research Technician III, Driftmier Engineering Center at the University of Georgia. All standardized curves were verified with a known concentration of a given compound within the bounds of the curve. Standard curves for xylose and glucose are shown in figures A.2 and A.3. Table A.1 shows the HPLC retention times for various compounds measured in this report.

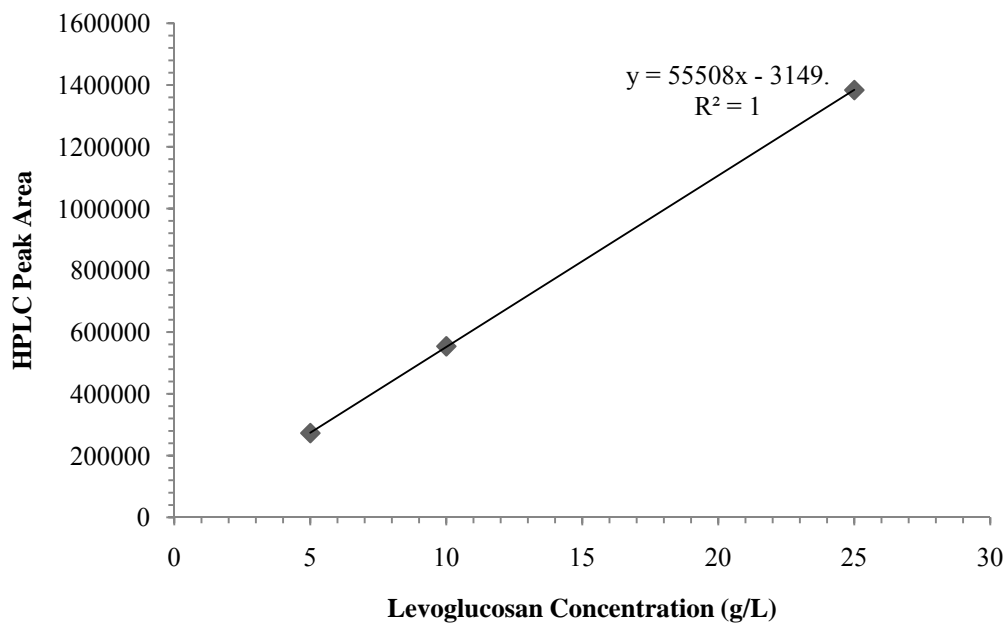


Figure A.1. Levoglucosan standard curve for HPLC analysis, 5-25 g/L

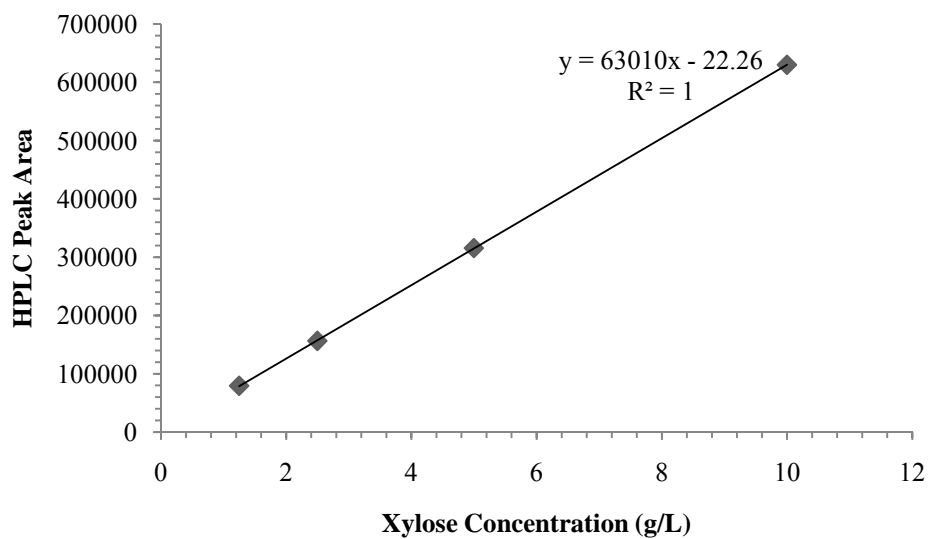


Figure A.2. Xylose standard curve for HPLC analysis, 1.25-10 g/L

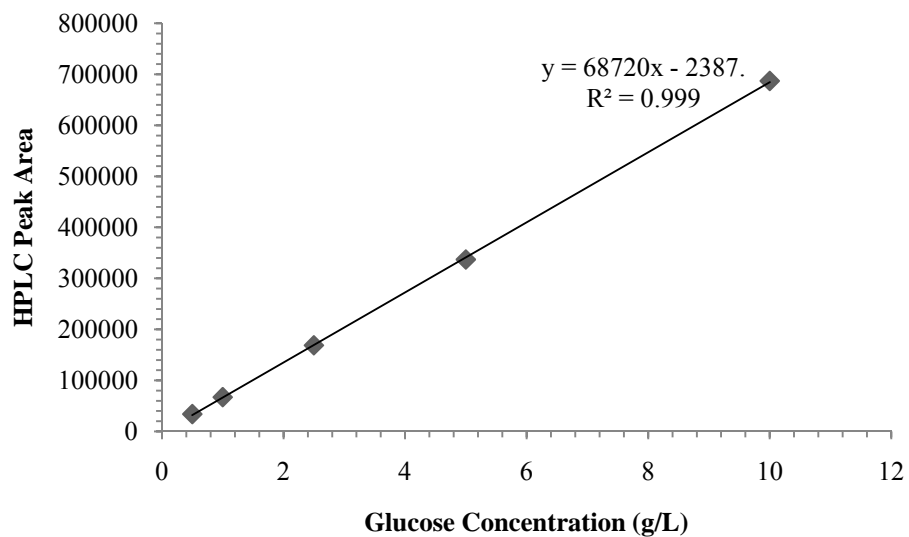


Figure A.3. Glucose standard curve for HPLC analysis, 0.5–10 g/L

Table A.1 HPLC retention times

Compound	Retention Time (min.)
Acetate	16.74
Ethanol	22.98
Furfural	47.2
Glucose	10.57
5-HMF	34.3
Levoglucozan	14.4
Xylose	11.35

## APPENDIX B

### COMPLETE ACID HYDROLYSIS CALCULATIONS

Due to the relative insolubility of xylan, HPLC analysis could not be used to quantify xylan concentrations directly. Change in xylan concentration was determined as a function of the change in xylose concentration. The National Renewable Energy Laboratory (NREL) method “Determination of sugars, byproducts, and degradation products in liquid fraction process samples” published in January 2008. Xylan samples of various concentrations were reacted with liquid sulfuric acid at 120 °C for 1 hr. Xylose samples of corresponding concentration were also reacted with the same liquid acid to account for any further decomposition to secondary products. The following equations were used to determine the content of xylose per unit of xylan.

$$\% R_{\text{xylose}} = \left( \frac{C_{\text{xylose HPLC}}}{C_{\text{xylose}}} \right) \times 100\%$$

$$C_x = \left( \frac{C_{\text{HPLC}} \times \text{dilution factor}}{\% R_{\text{avg. xylose}} / 100} \right)$$

$\% R_{\text{xylose}}$  = percent of xylose recovered from hydrolysis of xylose standard

$\% R_{\text{avg. xylose}}$  = average  $\% R_{\text{xylose}}$  of all trials

$C_{\text{xylose HPLC}}$  = HPLC measured concentration of xylose after xylose standard hydrolysis

$C_{\text{xylose}}$  = known concentration of xylose before hydrolysis

$C_x$  = corrected xylose concentration in the hydrolyzed xylan sample

$C_{\text{HPLC}}$  = HPLC measured concentration of xylose after xylan hydrolysis

Table B.1 Xylose recovery and xylan hydrolysis data for the calculation of xylose content

Sugar	C <sub>xylose</sub> (g/L)	C <sub>xylose HPLC</sub> (g/L)	% R <sub>xylose</sub>	Sugar	C <sub>xylan</sub> (g/L)	C <sub>HPLC</sub> x dilution factor (g/L)	C <sub>x</sub> (g/L)
Xylose A1	9.983	9.035	90.5%	Xylan A1	10	6.164	7.41
Xylose A2	10.023	7.196	71.8%	Xylan A2	10	5.971	7.18
Xylose A3	9.83	8.572	87.2%	Xylan A3	10	7.06	8.49
AVG % R <sub>xylose</sub>			83.2%	AVG C <sub>x</sub> (g/L)			7.69
Xylose B2	24.81	20.884	84.2%	Xylan B1	25	14.714	17.74
Xylose B2	25.05	20.476	81.7%	Xylan B2	25	15.53	18.72
AVG % R <sub>xylose</sub>			83.0%	AVG C <sub>x</sub> (g/L)			18.23
Xylose C	33.55	28.982	86.4%	Xylan C	35	20.2	23.38
Xylose D1	51.09	43.27	84.7%	Xylan D1	50	30.57	37.23
Xylose D2	49.82	39.62	79.5%	Xylan D2	50	30.89	37.62
AVG % R <sub>xylose</sub>			82.1%	AVG C <sub>x</sub> (g/L)			37.43

The total xylose content per unit xylan was calculated as an overall average of the average xylose content at each of the four initial xylan concentrations shown in table B.2.

The % xylose value is in terms of grams xylose produced from g xylan measured.

Table B.2 Average xylose content per unit xylan

$C_{\text{xylan}}$ (g/L)	AVG $C_x$ (g/L)	% Xylose
10	7.69	76.9%
25	18.23	72.9%
35	23.38	66.8%
50	37.43	74.9%
	<b>AVG</b>	<b>72.9%</b>